

The down-wind change of aeolian sand transport over a beach

Egmond aan Zee, the Netherlands

MSc thesis Earth Surface and Water,
Coastal dynamics and River systems

Author: J.D. Bergsma
Student number: 3819213
Supervisors: W. de Winter MSc, Prof. Dr. B.G. Ruessink
Second version: May 3, 2016

Utrecht University
Department of Physical Geography
Faculty of Geosciences



Abstract

High coastal dunes are vital to protect the hinterland from marine flooding during storms. To preserve these dune systems, insight into their erosion and growth is important. In previous years, research mainly focused on dune erosion. In recent years, there has been a substantial interest in the growth of the dune areas. At sandy beaches, aeolian wind-blown sand transport ensures the return of sand towards the dunes at a slow pace, i.e. days to months. Aeolian sand transport fluxes arise over a sandy beach in down-wind distance, from the top of the swash zone towards the dune area. At sandy beaches, aeolian sand transport rate depends on the wind climate and the surface parameters.

This research report is based on field data with short timescales, i.e. minutes to hours, at a sandy beach located south of Egmond aan Zee, the Netherlands, and focuses on how aeolian sand transport fluxes vary in down-wind direction over a bar-trough beach towards the dune area. The main aim of this research is to give more insight in how aeolian mass fluxes vary over the beach and to detect which factor has the most influence on aeolian mass fluxes in down-wind distance. During the field campaigns, aeolian sand fluxes were measured using Modified Wilson and Cooke (MWAC) sediment catchers to quantify the total mass flux. To measure the wind speed and direction, cup anemometers and sonic anemometers were used during the field campaign.

This research shows that a beach area can be divided into three sub-areas, where on each part of the beach unique factors increase or limit aeolian sand transport in down-wind direction. At the intertidal area it is observed that morphology limits aeolian sand transport, while the wind speed is the most important factor to start aeolian sand transport. At the upper beach, it is shown that the conditions to start or to continue aeolian sand transport are most favourable. The morphology ensures for limiting influence, while the combination of fetch length and wind speed ensures for most increase in aeolian mass flux. At the dune foot, it is noticed that the morphology is slightly more unfavourable than at the upper beach area. It is also indicated that during oblique wind conditions the wind speed is relatively lower at the dune foot than at the intertidal beach and the upper beach area. The wind direction is most important at the dune foot, because the wind direction ensures that the fetch is long enough to increase to its maximum.

In order to give better predictions for aeolian sand transport towards the dunes during model studies, there must be considered that there are several factors that increase or limit aeolian sand transport which alternate one another over the beach. Furthermore, in the results is shown that the wind speed decreases near the dunes during oblique wind directions, which might influence the amount of aeolian sand transport towards the dunes. Therefore all these different increasing or limiting parameters should be taken into account when predicting aeolian sand transport over the beach towards the dunes.

Table of contents and list of figures and tables

Abstract	3
1. Introduction.....	8
2. Literature review	9
2.1 Aeolian processes.....	9
2.2 Fetch effect.....	10
2.3 Morphology.....	12
2.4 Research question, objectives and hypotheses	13
2.4.1 Research question and objective	13
2.4.2 Hypotheses.....	14
3. Materials and methods	16
3.1 Study area.....	16
3.2 Data collection.....	17
3.2.1 MWAC sediment catchers	17
3.2.2 Wind speed and direction	18
3.2.3 Beach morphology.....	19
3.2.4 Surface moisture content.....	19
3.2.5 Grain size	19
3.3 Data processing	20
3.3.1 Aeolian mass flux.....	20
3.3.2 Wind speed corrections.....	20
3.3.3 Calibration Theta probes	21
3.3.4 Sieving process	22
3.4 Data analysis.....	23
3.4.1 Start point of aeolian mass fluxes	23
3.4.2 Linking wind speeds.....	23
3.4.3 Grain size distribution	23
3.5 Measurement locations and meteorological conditions	23
4. Results	30
4.1 Fetch length and aeolian sand transport	30
4.1.1 Cross-shore fetch conditions.....	30
4.1.2 Longshore fetch conditions	31
4.2 Varying wind climate conditions	32
4.2.1 Wind speed.....	32
4.2.2 Wind direction.....	33
4.3 Morphology.....	35

4.3.1	Down-wind fetch relations	36
4.3.2	Morphological relations	40
4.3.3	Beach profile variation	41
5.	Discussion	44
5.1	Influence of the fetch length	44
5.1.1	Cross-shore fetch length	44
5.1.2	Longshore fetch length.....	45
5.2	Influence of the wind conditions.....	45
5.2.1	Cross-shore wind measurements.....	46
5.2.2	Longshore wind measurements	47
5.2.3	External wind measurements.....	48
5.3	Influence of the morphology	48
5.3.1	Intertidal beach area	49
5.3.2	Upper beach area	50
5.3.3	Dune foot area.....	50
5.3.4	Morphology variations through time	51
6.	Conclusions.....	52
	Acknowledgements	53
	References.....	54
	Appendix, additional figures	56

Figure 1: Schematic diagram of the different aeolian sediment transport mechanisms (after; Nickling and Neuman (2009)).	10
Figure 2: Basic description of the fetch effect on a beach. F is the fetch effect, F_c is the critical fetch length, F_m is the maximum fetch length depending on the characteristics of the beach and tide and α is the incoming wind angle. Two different areas are indicated. The intertidal beach area, this area is affected by the vertical tidal displacement. The upper beach area, which consist mostly of dry sand and is the zone between the intertidal beach area and the dune foot area (after; Bauer and Davidson-Arnott, 2002).	11
Figure 3: Aeolian mass flux variation, i.e. fetch length, in down-wind distance during different wind speed conditions. For the first two wind conditions the critical fetch length appears, while for the third wind speed this critical fetch length is not reached at the maximum fetch length of the beach (after Bauer and Davidson-Arnott, 2002; Davidson-Arnott and Law, 1990).....	11
Figure 4: Basic description of fetch segmentation (F) for different vertical tidal displacements at intertidal bar-trough topography. MSL = Mean sea level. The grey surfaces show time-varying areas where no aeolian sand transport occurs. This is mostly at moist surfaces, as a consequence of the fluctuating water table. Situation A, B and C show different tidal conditions, with varying lengths of the fetch segments (after; Anthony et al., 2009: profile of Leffrinckoucke, 08/10/2001).	12
Figure 5: The study site (the red rectangle) at the Western Dutch coast line, South of Egmond aan Zee and the nearby weather station de Kooy, Den Helder (Google Earth, 2015).	16

Figure 6: An example of the field site during aeolian sand transport at the South side of the Argus Tower at Egmond aan Zee on October 21, 2015. The field work area has a length of about 250 m in the longshore direction and is about 60 – 120 m in beach width depending on the vertical tidal fluctuation. 17

Figure 7: The Modified Wilson and Cooke sediment catcher (after Sterk and Raats, 1996). 18

Figure 8: A; the wind mast containing 5 cup anemometers at logarithmic scale and on top a wind vane. B; a sonic anemometer. 19

Figure 9: A; the 11 different sieves on top of each other at the shaking device. B; Scale where all the individual sieves are weighted on, before and after the sand samples are put into the sieves. 22

Figure 10: A; the locations of the different measurements at April 2. B; the wind speeds (colour lines) and wind directions (black line) for one locations. The vertical solid lines 1 and 2 indicate the starting and ending time of the run that is done at the intertidal and upper beach array during the event. ... 27

Figure 11: A; the locations of the different measurements at October 7. B; the wind speeds (colour lines) and wind directions (black lines) for different locations. The vertical lines indicate the start or end time of the different runs that are done during the event. The dotted lines indicate the measurements at the dune foot, while the solid lines indicate the measurements at the upper beach. The numbers 1, 2 and 4 indicate the start of the measurements at the dune foot, while the numbers 5, 8 and 9 indicate the end of the measurements at the dune foot. The numbers 3, 6, 11 and 12 indicate the start of the measurements at the upper beach, whereas the numbers 7, 10, 13 and 14 indicate the end of the measurements at the dune foot. 28

Figure 12: A; the locations of the different measurements at October 21. B; the wind speeds (colour lines) and wind directions (black line) for different locations. The vertical dotted lines 1 and 2 indicate the starting and ending time of the run that is done at the dune foot during the event. 28

Figure 13: A; the locations of the different measurements at October 22. B; the wind speeds (colour lines) and wind directions (black lines) for different locations. The vertical lines indicate the start or end time of the different runs that are done during the event. The dotted lines indicate the measurements at the dune foot, while the solid lines indicate the measurements at the intertidal and upper beach. The numbers 2 and 4 indicate the start and end of the measurements at the dune foot, while the numbers 1 and 3 indicate the start and end of the measurements at the intertidal and upper beach. 29

Figure 14: A; the locations of the different measurements at October 24. B; the wind speeds (colour lines) and wind directions (black lines) for different locations. The vertical lines indicate the start or end time of the different runs that are done during the event. The dotted lines indicate the measurements at the dune foot, while the solid lines indicate the measurements at the intertidal and upper beach. The numbers 1 and 5 indicate the start and end of the measurements at the dune foot. The numbers 2 and 3 indicate the start of the measurements at the intertidal and upper beach, while the numbers 4 and 6 indicate the end of the measurements at the intertidal and upper beach. 29

Figure 15: All aeolian mass flux measurements that were done in cross-shore direction over the beach during 2 events. For the measurement arrays, see Figure 10 A and Figure 13 A. 30

Figure 16: All aeolian mass flux measurements that were done in longshore direction over the beach. A; all aeolian mass fluxes measured at the dune foot during 4 events. B; all aeolian mass fluxes measured at the upper beach during 2 events. For the measurement arrays, see Figure 11 A to Figure 14 A. 32

Figure 17: All the measured cross-shore and longshore wind conditions with their aeolian mass flux for each individual sediment catcher of the 5 events on a semi-logarithmic scale. A circle (O) means that the measurements were taken in cross-shore direction over the beach, while an asterisk (*) means that the measurements were done in longshore direction over the beach. 33

Figure 18: An overview of how aeolian mass fluxes (green line) react on different profiles over the beach with the three morphological parameters incorporated; the beach height, the surface moisture content and the grain size. The surface moisture content is measured before and after the run (dark blue = before, light blue = after) and also the grain size is measured before and after the run (red = before, pink = after). The grain size is divided in three different classes: top = D_{10} , middle = D_{50} , bottom = D_{90} . A; The three different measurement profiles that will be shown in more detail in Figure 18 B, C and D. B; Beach profile over the upper beach area in longshore direction. C; Beach profile at the dune foot area in longshore direction. D; Beach profile over the intertidal beach, the upper beach and the dune trough in cross-shore direction. 39

Figure 19: A; aeolian mass fluxes plotted against the mean grain size (D_{50}) for different measurements before and after a run was started. B; aeolian mass fluxes plotted against the surface moisture content for different measurements before and after a run was started. 41

Figure 20: An overview of the change in beach profile through time for the different time periods used for the grain size distribution through time. 42

Figure 21: An overview of the grain size class variation through time, measurements were taken from October 19 to October 24 and from October 27 to October 29. A; the grain size variation through time for the D_{10} values. B; the grain size variation through time for the D_{50} values. C; the grain size variation through time for the D_{90} values. In the legend the variation values are in μm 43

Figure 22: An overview of the grain size distribution achieved by the inverse distance weighting (IDW) interpolation for all the grain size class measurements done between October 19 and October 24. A; the grain size distribution for the D_{10} class. B; the grain size distribution for the D_{50} class. C; the grain size distribution for the D_{90} class. All grain size values are in μm 56

Figure 23: An overview of the grain size distribution achieved by the inverse distance weighting (IDW) interpolation for all the grain size class measurements done between October 27 and October 29. A; the grain size distribution for the D_{10} class. B; the grain size distribution for the D_{50} class. C; the grain size distribution for the D_{90} class. All grain size values are in μm 56

Table 1: Overview of the different arrays and their locations on the beach, the direction of positioning and the maximum of sediment catchers than could be placed during the fieldwork campaigns..... 24

Table 2: An overview of the 5 measurement days, the MWAC sediment catchers and their locations, the mean wind speeds and the mean wind directions. 24

Table 3: An overview of the measured hourly average wind speeds and wind conditions at de Kooy, Den Helder during the measurements at the study site..... 25

1. Introduction

High coastal dunes are vital to protect the hinterland from marine flooding during storms. To preserve these dune systems, insight into dune erosion and dune growth processes are important. In previous years, research mainly focused on dune erosion. In recent years, there has been a substantial interest in the growth of dune areas. The condition of dunes depends on the impact strength of the previous storm and the ability of dunes to recover by aeolian sand transport fluxes (Houser, 2009). At sandy beaches, aeolian wind-blown sand transport ensures for the return of sand towards the dunes at a slow pace, i.e. days to months.

There is a large scale of spatial variability of aeolian sand transport fluxes over a sandy beach in down-wind distance, from the swash zone towards the dune area. At sandy beaches, the rate of aeolian sand transport depends on the wind climate and the surface parameters. The temporal and spatial parameters at the beach surface depend on the lag deposits, the grain size, the moisture content and the topography of the beach (Anthony et al., 2009; Bauer and Davidson-Arnott, 2002).

Most parameters which affect aeolian sand transport are known. However, all the parameters in the aeolian process need to be understood before aeolian sand transport can be investigated quantitatively (Davidson-Arnott and Law, 1990). At present, the interactions between all the previously mentioned parameters are still not entirely understood (Anthony et al., 2009; Bauer et al., 2009; de Vries et al., 2014).

In order to give a better prediction of aeolian sand transport over a beach in down-wind distance, the wind climate and the surface parameters need to be better understood. Therefore, this research will focus on which parameters have the most influence on aeolian sand transport at the different parts of the beach: the lower beach area, the upper beach area and the dune foot area.

This research report is based on field data with short timescales, i.e. minutes to hours, at a sandy beach and focuses on how aeolian sand transport fluxes vary in down-wind direction over a bar-trough beach towards the dune area. The measurements for this research are realized at the beach of Egmond aan Zee, during two field campaigns in the spring and autumn of 2015.

In the literature review, current knowledge and knowledge gaps are identified. Based on the review, research questions and hypotheses are given. Then the study site and methods are described, followed by the results, discussion, and conclusions.

2. Literature review

To understand the basic principles for aeolian sand transport over a beach the aeolian process is explained, together with the terms that are used to describe aeolian sand transport in the literature. Whereafter, the parameters that might influence aeolian sand transport in down-wind direction are described, i.e. the wind conditions and the morphology, along with the remaining uncertainties brought up in the literature. This is followed by the research questions, objectives and hypothesis of this thesis.

2.1 Aeolian processes

Aeolian sand transport is the process of transporting sand particles due to the uplifting force of wind. At sandy beaches, aeolian sand transport ensures for the return of sand towards the dunes at a slow pace, i.e. days to months. To transport sand towards the dune area, onshore perpendicular or oblique winds are essential (Bauer and Davidson-Arnott, 2002; Davidson-Arnott and Law, 1990). During onshore or oblique wind directions, potential aeolian sand transport starts at the swash line, where the sea surface ends, because no sediment is introduced from upwind (Bauer and Davidson-Arnott, 2002; Davidson-Arnott and Law, 1990).

To start aeolian sand transport the wind speed must exceed the critical shear stress, also referred to as the threshold of movement, whereupon sand particles can be transported in down-wind direction (Bauer and Davidson-Arnott, 2002; Bauer et al., 2009). The movement of sand particles in down-wind direction can occur in four different ways (see Figure 1). The first way is by the 'creep' process. During this process, sand particles will roll and remain in contact with the beach surface (Bagnold, 1941). The second way in which sand particles move is by making small hops, called 'reptation' (Anderson, 1987). When these small hops increase to larger leaps it is named 'saltation'. Turbulence in the wind can cause sand particles to remain in the air, which is then called 'suspension' (Bagnold, 1941). The moment the saltating grains hit the beach surface, the particles can eject resisting grains into the air, called the 'cascade' process. This positive feedback process increases the number of saltating grains in aeolian sand transport (Bauer et al., 2009). As a result of the increasing number of saltating grains, an exponential increase in transport in down-wind direction is observed, provided that the wind speed remains strong enough to keep the sand particles in motion (Bauer et al., 2009). This process continues until the saturation rate of the gusting wind is reached, i.e. when the wind carries its maximum amount of aeolian sand (Bauer et al., 2009; Davidson-Arnott and Law, 1990).

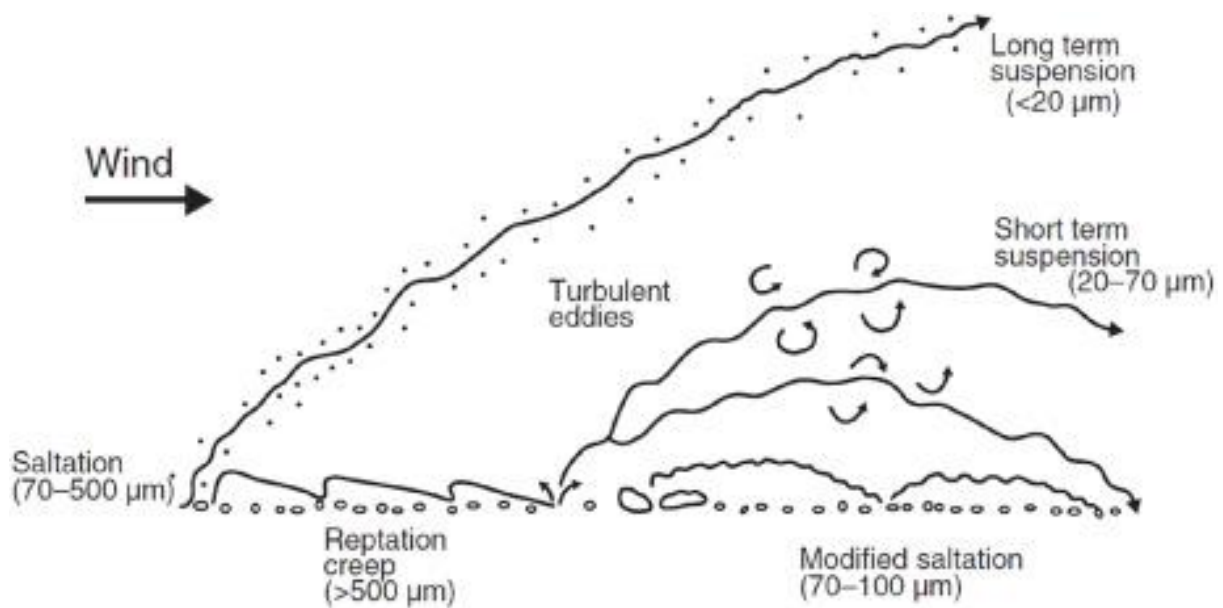


Figure 1: Schematic diagram of the different aeolian sediment transport mechanisms (after; Nickling and Neuman (2009)).

2.2 Fetch effect

The 'fetch effect' is introduced to describe the aeolian process in aeolian sand transport studies. The fetch effect is the increase in aeolian sand transport in down-wind direction of the wind path (Gillette et al., 1996) and describes the aeolian process off non-existent aeolian sand transport at the top of the swash zone, followed by an increase in aeolian sand transport towards the foredune area (Bauer and Davidson-Arnott, 2002). This process can continue until it reaches a maximum equilibrium rate at a certain down-wind distance at the beach (section 2.1) (Bauer et al., 2009; Davidson-Arnott and Law, 1990). In aeolian sand transport studies, the fetch (F) at a beach is the distance from a reference point, here the sea, up to a certain point in the wind path (Figure 2) (Bauer and Davidson-Arnott, 2002). The fetch is used to determine aeolian sand transport rate at that specific location at the beach, which is a result of the maximum fetch length (F_m) and the critical fetch length (F_c). The maximum fetch is affected by the width of the beach (W) and the incoming wind angle (α), which can be shore perpendicular, oblique or shore parallel. The location from which the equilibrium rate first appears is called the critical fetch length, which is the maximum transport capacity of the gusting wind. The critical fetch can arise under shore perpendicular or oblique wind directions, provided that the wind is strong enough or that the beach width is wide enough to overrule limiting factors. When the wind direction is shore parallel, the fetch becomes infinite, which will result in a critical fetch length down-wind, even though the wind is less strong compared to the shore perpendicular or oblique wind speeds (Bauer et al., 2009).

The critical fetch length depends mostly on the wind conditions as stated by Davidson-Arnott and Law (1990). They found that during higher wind speeds the critical fetch length appeared further in

down-wind direction (Figure 3), since it takes longer before the equilibrium of the gusting wind is reached. They were the first who recognized the importance of the fact that the maximum fetch length can increase when the wind angle becomes more oblique. In previous studies multiple aeolian mass flux measurements were taken in down-wind distance (Anthony et al., 2009; Bauer et al., 2012, 2009; Davidson-Arnott et al., 2005). However, there is a lack of understanding how and by what aeolian mass fluxes are influenced over the beach and no good correlations can be made between the intertidal area, the upper beach area and the dune foot area.

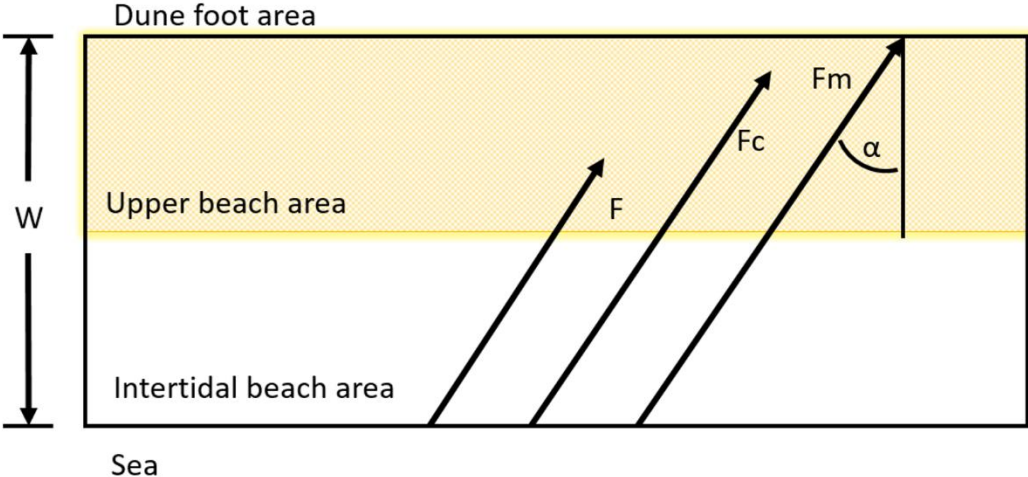


Figure 2: Basic description of the fetch effect on a beach. F is the fetch effect, F_c is the critical fetch length, F_m is the maximum fetch length depending on the characteristics of the beach and tide and α is the incoming wind angle. Two different areas are indicated. The intertidal beach area, this area is affected by the vertical tidal displacement. The upper beach area, which consist mostly of dry sand and is the zone between the intertidal beach area and the dune foot area (after; Bauer and Davidson-Arnott, 2002).

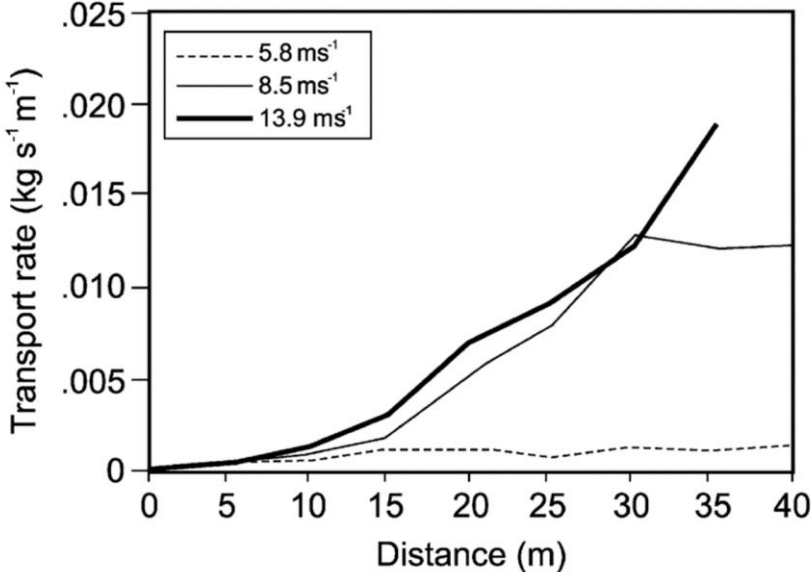


Figure 3: Aeolian mass flux variation, i.e. fetch length, in down-wind distance during different wind speed conditions. For the first two wind conditions the critical fetch length appears, while for the third wind speed this critical fetch length is not reached at the maximum fetch length of the beach (after Bauer and Davidson-Arnott, 2002; Davidson-Arnott and Law, 1990).

2.3 Morphology

In the past decades, most aeolian research was realized on flat beaches, where aeolian sand transport flux can increase rapidly in down-wind direction (Bauer et al., 2009; Sherman and Li, 2012). However, aeolian sand transport fluxes act differently on bar-trough beaches as is observed by Anthony et al. (2009), Davidson-Arnott and Law (1990) and Vanhée et al. (2002). In their research they found that aeolian sand transport flux depends on the strongly varying surface moisture content across a bar-trough beach and that aeolian sand transport is slowed down or limited over a bar-trough topography. It is also noticed that at a bar-trough beach the surface moisture content is strongly dependent on the fluctuating bar-trough elevations, and that at bars lower surface moisture contents are found than in troughs (Oblinger and Anthony, 2008). The high surface moisture contents in the trough ensure a reduction in the cascade effect, due to the increased inter-particle cohesion (Bauer et al., 2009). As a result, the critical fetch length will be reached further in down-wind direction or is not reached at all when the fetch is limited by the maximum fetch length. Anthony et al. (2009) state that due to the bar-trough system at the intertidal beach, different fetch segments appear (Figure 4), so the uptake of particles into aeolian sand transport must start over when it reaches a moist surface. They also indicated that the uptake of sand particles is complicated by the variation in wind patterns above the bar-trough topography, because the wind pattern has to expand in the trough and therefore the wind speeds decreases. Based on the previous mentioned research it is indicated that troughs act as efficient sand interceptors, which will decrease the maximum fetch length over the entire beach. It also can be noted that there is probably a high correlation between the increase in surface moisture content near lower areas of the beach profile, on the decrease in aeolian sand transport fluxes over a beach.

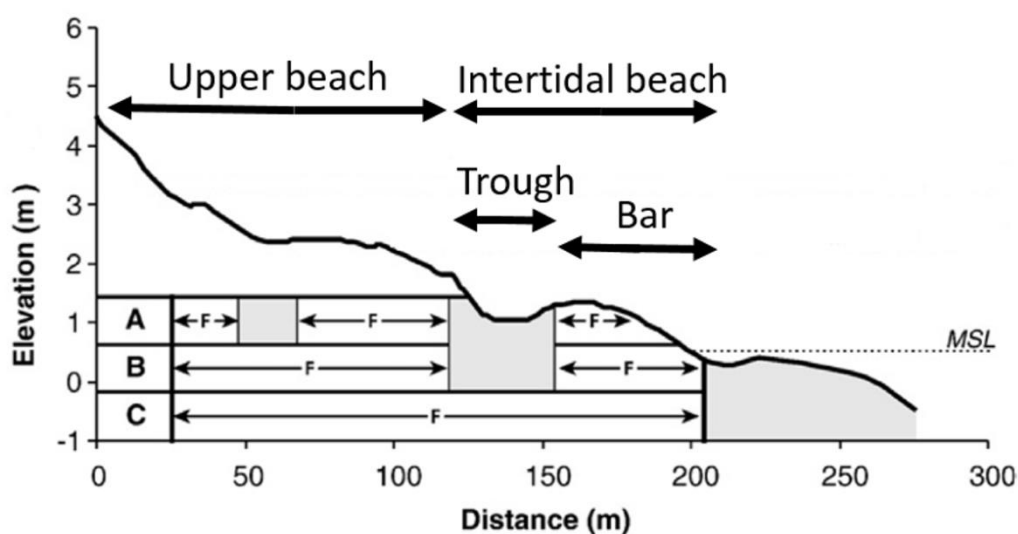


Figure 4: Basic description of fetch segmentation (F) for different vertical tidal displacements at intertidal bar-trough topography. MSL = Mean sea level. The grey surfaces show time-varying areas where no aeolian sand transport occurs. This is mostly at moist surfaces, as a consequence of the fluctuating water table. Situation A, B and C show different tidal conditions, with varying lengths of the fetch segments (after; Anthony et al., 2009: profile of Leffrinckoucke, 08/10/2001).

Besides the surface moisture content, also other surface parameters can influence the fetch length such as grain size distribution, surface roughness, beach slope, bedform development and the topography of the beach (Anthony et al., 2009; Bauer et al., 2009). All these surface parameters can limit aeolian sand transport in down-wind distance and are highly variable in space and time (Anthony et al., 2009; Bauer and Davidson-Arnott, 2002; Bauer et al., 2009; Gillette et al., 1996). However, in what amount these surface parameters influence aeolian sand transport in down-wind direction at the different beach areas is still not entirely clear.

2.4 Research question, objectives and hypotheses

2.4.1 Research question and objective

In previous research a focus has been made on aeolian sand transport and how it reacts on limiting factors. However, there are still uncertainties in how aeolian sand is transported over the entire beach and which factors ensure an increase or a decrease in aeolian mass flux at different parts of the beach. The main aim of this research is to give more insight in how aeolian mass fluxes vary over the beach and to detect which factor has the most influence on aeolian mass fluxes in down-wind distance, so a better prediction for the growth of the dunes can be made. Therefore, it allows answering the following research question: *Which factors influence aeolian transport patterns on a sandy beach and what are their separate consequences at the different parts over the beach?*

There are multiple factors that influence aeolian sand transport. Therefore several factors will be isolated to detect the effect of down-wind change in aeolian mass flux for the different areas over the beach. The research question is divided into three consecutive research topics: the relation between fetch length and aeolian mass flux (1), the influence of wind climate on aeolian mass flux (2) and the influence of morphology on aeolian mass flux (3). The general scheme of this thesis is by answering the three sub-questions, which are:

1. What is the relation between fetch length and aeolian mass flux?
2. How do the longshore and cross-shore wind conditions affect aeolian mass flux in down-wind distance?
3. How does the morphology affect aeolian mass flux in down-wind distance?

To answer the first research topic a distinction is made between the longshore measurements and the cross-shore measurements that were taken during the events at the different parts over the beach. When the interaction between fetch length and aeolian mass flux is clear, the effects of the wind conditions are incorporated to answer the second sub-question, and again a distinction is made between longshore and cross-shore measurements at the different parts over the beach.

Furthermore, there will be looked if it is possible to use the wind data of the nearby weather station to predict aeolian mass flux over the beach. In order to find out if these known wind conditions are suitable enough to use during model studies. To answer the third sub-question, three features of the morphology will be considered. These features will be the variation in elevation, the variation in surface moisture content and the variation in grain size in down-wind distance. Again a distinction is made between the longshore and the cross-shore measurements that were taken during the events at the different parts over the beach. The change in morphology will also be examined through time and how these variations might influence aeolian mass flux in down-wind direction for the whole field site area.

2.4.2 Hypotheses

Based on the literature review the following hypotheses are made for the research question and for the three consecutive topics.

In case of the first sub-question, it is expected that during the cross-shore measurements the start of aeolian sand transport in down-wind direction is observed as is described by Davidson-Arnott and Law (1990). Therefore it is expected to find an increase in aeolian mass flux in down-wind direction. The same relation as is described by Davidson-Arnott and Law (1990) is expected to be found for the longshore measurements, but then at the equilibrium state, because there is a longer fetch path to increase aeolian sand transport. It is also expected that when two longshore measurements are made during the same event, equal equilibrium relations are found.

The hypothesis for the second sub-question is that during cross-shore measurements it is expected that the wind speed plays the most important role in the start of aeolian sand transport in down-wind distance (Davidson-Arnott and Law, 1990). Due to the wind direction, which will be onshore or cross-shore, aeolian sediment transport starts increasing after it crossed the swash line. However, the wind has to be strong enough to exceed all factors that decrease aeolian sand transport at the intertidal beach (Anthony et al., 2009). Thus, when all limiting factors are overruled and the wind is strong enough, aeolian sand transport arises in down-wind direction. Whereas, during the longshore measurements the wind direction probably has the most influence on the start of aeolian sand transport. Because even when the wind speed is low, aeolian sand transport may arise when there is a favourable wind direction, i.e. when the wind comes from longshore direction (Davidson-Arnott et al., 2005). Furthermore, the wind conditions of the nearby weather station will be compared with the measured wind data at the field site. In order to get more information if the wind data from the weather station is suitable to use for aeolian model studies to model the sand

transport fluxes over the beach towards the dunes. However, it is expected that the wind data is probably not locally enough to give a good prediction about aeolian mass flux at the different parts of the beach.

In case of the third sub-question, it is expected that the morphology will have the strongest influence on the intertidal beach area (Anthony et al., 2009; Vanhée et al., 2002). The intertidal beach is characterized by a relatively large variation in height which ensures that the surface moisture content increases (Anthony et al., 2009) and that grain size is relatively larger (Pedreros et al., 1996). At the upper beach area and dune foot area the morphology will have less influence on aeolian mass flux, because there is a small variation in the surface height, and therefore a small variation in surface moisture content and grain size (Oblinger and Anthony, 2008). It can also be expected that the variation in beach morphology through time might also have a limiting influence on aeolian mass flux in down-wind distance, because the grains will be mixed with one another and therefore it will retain the sorting process of the grains (Pedreros et al., 1996).

To give a hypothesis for the main research question, it is expected that at the intertidal area there will be a lower aeolian mass flux than at the upper beach and the dune foot area (Davidson-Arnott and Law, 1990). At the intertidal beach the flux cannot develop sufficiently, due to the limiting fetch length and the high surface moisture content (Anthony et al., 2009). While, at the higher part of the beach, i.e. the upper beach and dune foot, the surface moisture content is lower and the fetch length can increase sufficiently. As a result that this area is more suitable for aeolian mass fluxes to arise (Davidson-Arnott et al., 2005).

3. Materials and methods

3.1 Study area

Two field campaigns were conducted on a narrow sandy beach at the western Dutch coast line during spring 2015, from March 23 to April 2, and during autumn 2015, from September 22 to October 30. The field site is located at the south side of the Argus Tower and this area has often been used during previous fieldwork campaigns in combination with the surveillance of the Argus Tower (Figure 5) (Holman and Stanley, 2007; Quartel et al., 2007). The field campaigns were conducted by a team from the department physical geography of Utrecht University, with the aim to provide better predictions of aeolian processes from the beach towards the dunes.

The field site has a semi-diurnal tidal regime and is wave dominated with a predominant wind direction from the southwest, whereas the largest storms occur during north-western winds. The beach is gently sloped and has a bar-trough morphology with 1 intertidal sandbar. The foredunes are about 25 m in height and the dune area is 1 – 2 km in width from the beach up to the hinterland. Due to the large erosion that occurs during storms, the foredunes are planted with marram grass. The field work area is in longshore direction about 250 m in length and the beach width varies between 60 – 120 m (Figure 6). The beach consists out of well sorted fine quartz sand ($D_{50} = 279 \mu\text{m}$, $D_{10} = 207 \mu\text{m}$, $D_{90} = 376 \mu\text{m}$).

Storms are frequent during autumn, winter and spring in the Netherlands, thus the fieldwork campaign was planned for the spring and autumn of 2015. During these field campaigns, an extensive data set was gathered including aeolian sand transport fluxes, the beach topography, the tidal signal (the varying width of the beach) and the surface moisture content, during perpendicular and oblique onshore and longshore wind events.

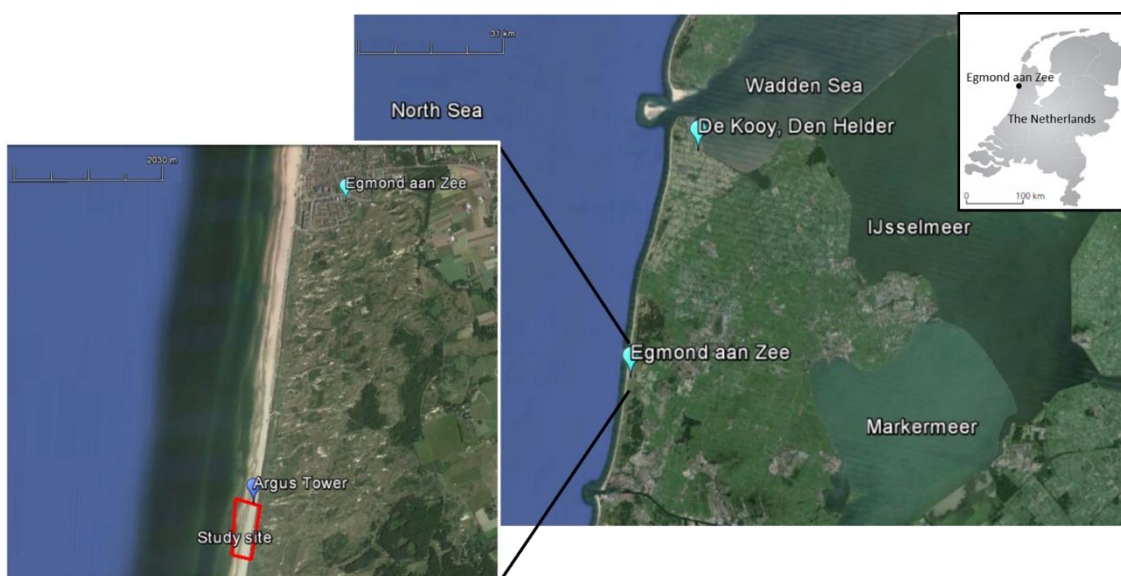


Figure 5: The study site (the red rectangle) at the Western Dutch coast line, South of Egmond aan Zee and the nearby weather station de Kooy, Den Helder (Google Earth, 2015).

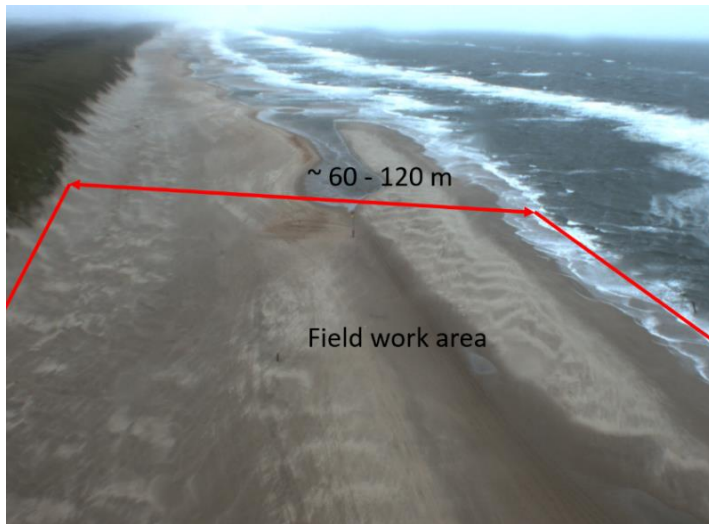


Figure 6: An example of the field site during aeolian sand transport at the South side of the Argus Tower at Egmond aan Zee on October 21, 2015. The field work area has a length of about 250 m in the longshore direction and is about 60 – 120 m in beach width depending on the vertical tidal fluctuation.

3.2 Data collection

3.2.1 MWAC sediment catchers

During the field campaigns, aeolian sand fluxes were measured using Modified Wilson and Cooke (MWAC) sediment catchers to quantify the total mass flux (Sterk and Raats, 1996; Sterk et al., 2012). These sediment catchers trap sediment on 6 different heights, at approximately 0.05, 0.12, 0.17, 0.23, 0.36 and 0.61 meter above the beach surface and were attached to a frame (Figure 7). The height of the trap with respect to the beach surface was measured individually for each MWAC sediment catcher for each event, and the measurement error is approximately 1 to 3 millimeter. The trap consists of a plastic bottle with two glass tubes. The bottles were installed vertically, so the inlet and outlet of the glass tubes are oriented into the wind. The air, along with the sediment, enters the bottle through the inlet tube, while the outlet tube ensured that the air can escape the bottle after the sand has settled down in the bottle due to pressure stabilisation. In advance and afterwards the bottles were weighed, so the total trapped sediment could be determined and recalculated to a mass flux density for each height. A sail, attached to the sand catcher, ensured that the inlets of the tubes were positioned into the dominant wind direction. Special care was taken with the lower bottles, because a slight change in height above the bed can result in a large misprediction when the mass flux values for the first few centimeters above the bed are plotted (Ellis et al., 2009), therefore in the field the distance between the beach surface and the first bottle was measured before and after each run. During each event the bottles could be replaced for two to six times, depending on the measurement period, the measurement setup and the weather conditions. Also, for each run, the time at the start and at the end was noted (see Figure 10 B to Figure 14 B vertical black solid and dotted lines).

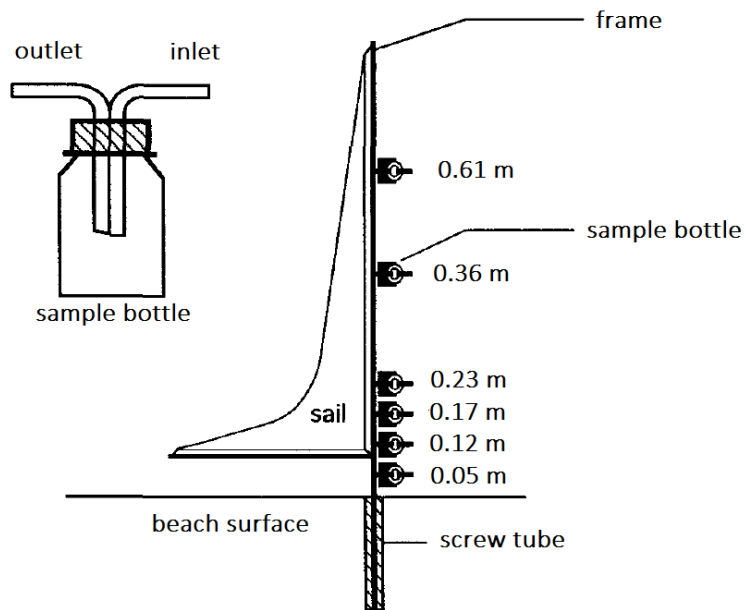


Figure 7: The Modified Wilson and Cooke sediment catcher (after Sterk and Raats, 1996).

3.2.2 Wind speed and direction

To measure the wind speed and direction, cup anemometers and sonic anemometers were used during the field campaign (Figure 8) (van Boxel et al., 2004; Walker, 2005). The cup anemometer gave an average wind speed and an average wind direction for every minute and the sonic anemometer measured a wind speed and wind direction every 0.1 second.

Wind mast

The 3-cup anemometers were attached to a mast which was positioned at the upper-beach at a fixed frame. Five cup anemometers were installed in the mast, at logarithmically distributed height intervals of approximately 0.13, 0.40, 0.63, 0.88 and 2.00 meter above the beach surface, and a wind vane was installed on top of the mast, at a height of approximately 2.15 meter. These heights were measured individually for each cup anemometer and wind vane for each event and the measurement error is approximately 1 to 3 millimeter. The wind vane was aligned on beach poles, so the measured wind direction by the wind vane can be corrected to the correct wind direction.

Sonic anemometers

The sonic anemometers were located near the MWAC sediment catchers and were also aligned on beach poles, so the wind direction measured by the sonic anemometer can be corrected for the right wind direction. All heights of the sonic anemometers were measured in the field and again the measurement error is around 1 to 3 millimeter.

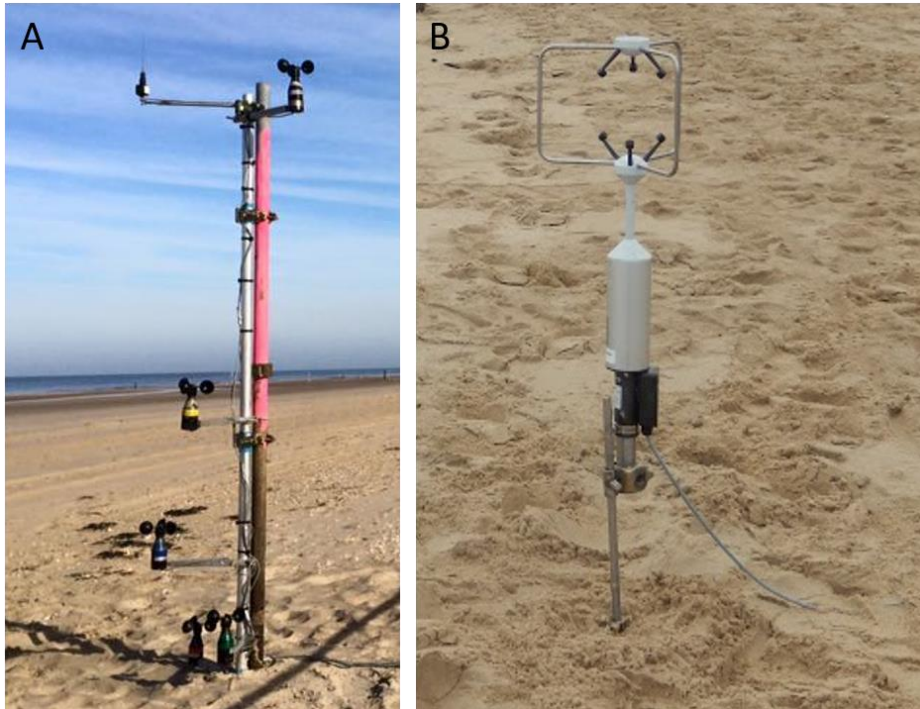


Figure 8: A; the wind mast containing 5 cup anemometers at logarithmic scale and on top a wind vane. B; a sonic anemometer.

3.2.3 Beach morphology

The beach profile and equipment were measured with a global positioning system (DGPS) device for each event. To get more morphological detail of a certain area at the field site, a wheel was detached beneath the DGPS, whereas a quad was used for larger morphological surfaces. Both methods resulted in information about the topography of the beach. The standard deviation was several millimeters, which is relatively small to the surrounding beach profile, but it ensures that individual bedforms are not displayed.

3.2.4 Surface moisture content

The surface moisture content was measured with a calibrated Delta-T Theta probe (Atherton et al., 2001; Edwards and Namikas, 2009; Oblinger and Anthony, 2008; Yang and Davidson-Arnott, 2005) next to the MWAC sediment catchers. The Theta probe was 2 cm long, so only the surface moisture content of the beach surface was estimated. To compensate for the measurement error 3 or 5 measurements were taken at each location, so the average was calculated whereupon the surface moisture content was determined.

3.2.5 Grain size

To get a better indication about the change in grain size over the beach through time, two different sorts of sand samples were taken. The first sand samples were taken from different

locations over the beach, in three arrays from the sea-side towards the dunes, at two days. As a result, an indication for the variation of grain size was made through time. The second set of sand samples was taken in front of the MWAC sediment catchers before and after the start of the run during aeolian sand transport events, thereafter an indication was made if the grain size changed during the event.

3.3 Data processing

3.3.1 Aeolian mass flux

The mass of the sediment from the MWAC sediment catcher sample bottles was determined from the weight of each single sample bottle before and after the event. These masses then were converted to a flux in three steps. First, the mass had to be corrected for the area of the inlet tube opening. Second, the mass was divided by the total measurement time and the third step was that the mass had to be corrected for the efficiency of the MWAC sediment catcher which was 0.35, so an aeolian sand flux could be calculated. These fluxes were plotted against the measured height relative to the beach surface. Through these data points a fit was made with the exponential curves (Ellis et al., 2009). Aeolian mass flux was then calculated by determining the area below the curve, which resulted in an aeolian mass flux at each location where a MWAC sediment catcher was positioned.

3.3.2 Wind speed corrections

To compare all the measured wind velocities with one another, the wind data first had to be corrected to wind speeds at an equal height of 0.9 meter. The correction for the cup anemometers was done in three steps (after van Rijn, 1990). First, the zero-velocity level (z_0) of each measurement day had to be calculated, by using the different speeds and heights of the cup anemometers. Where u_1 and z_1 were the wind speed and height of one cup anemometer and u_2 and z_2 were the wind speed and height of another cup anemometer, provided that the cup anemometers worked correctly during that measurement day.

$$z_0 = e^{\frac{u_1 - 2.5 \frac{u_1 - u_2}{2.5 \ln \frac{z_1}{z_2}} \ln z_1}{-2.5 \frac{u_1 - u_2}{2.5 \ln \frac{z_1}{z_2}}}} \quad (1)$$

Secondly, the shear velocity (u^*) of each wind measurement location has to be determined, by using the wind speed (u) and height (z) of each individual measurement location.

$$u^* = \frac{u}{2.5 \ln \frac{z}{z_0}} \quad (2)$$

The last step is to use the z_0 and the u^* to calculate the wind speed at a height of 0.9 meter. Where u_z is the wind speed at a height (z) of 0.9 m and κ is the Von Karman constant with a value of 0.4.

$$u_z = \frac{u^*}{\kappa} \ln \frac{z}{z_0} \quad (3)$$

All the measured wind speeds are corrected to a wind speed at a height of 0.9 meter, as described above, and were used in the rest of this report.

To correct the sonic anemometer data, first the raw measured data had to be rotated using the method of van Boxel et al. (2004). This method computes the three-dimensional wind vector from the high frequency sound pulses. After rotating the wind data, the wind data is further corrected as was done for the cup anemometers. However, the z_0 that was derived from the cup anemometers was also used to calculate the shear stress (equation 2), for each sonic anemometer at the same measurement day. This resulted in a corrected wind speed at a height of 0.9 meter, by using equation 3. Based on the corrected data, mean wind speed and direction of one individual minute was calculated. These values were used in the rest of this report.

3.3.3 Calibration Theta probes

The theta probe was calibrated two times by taking 30 sand samples at the start and the end of the second fieldwork campaign (Atherton et al., 2001; Edwards and Namikas, 2009; Oblinger and Anthony, 2008; Yang and Davidson-Arnott, 2005). All the sand samples that were collected for the calibration are dried. Drying of the sand samples was essential to determine the amount of water in the sand sample. The sand samples were put in aluminium trays and were dried for 24 hours in an oven at 105 °C. The weight of the aluminium trays, containing the sand, was measured before and after they were placed in the oven. As was the individual weight of each aluminium tray measured before and after the sand sample was placed in the oven, so a correction was made for the sand that remained in the aluminium trays. As a result, the gravimetric soil moisture content was determined from the change in weight through the evaporated water. A calibration curve was made for each Theta probe by plotting all the gravimetric soil moisture contents, gathered from the dried sand samples, and the mean Theta probe output, measured at the location of the sand sample. During the field campaign each Theta probe was calibrated two times, so the mean of these two calibrations was used for the individual Theta probe. The mean Theta probe outputs measured in front of each

MWAC sediment catcher were corrected with the calibration curve. As a result, the actual surface moisture content of the measurement location was found, which are used in the rest of this thesis.

3.3.4 Sieving process

All the grain size sand samples that were collected during the field work campaign are dried, so the samples could be sieved. To dry the sand samples, the sand remained in the plastic sac and was put in an oven at 70 °C for 72 hours. After drying the samples, the sand was sieved through 11 sieves that were placed on top of each other. The first sieve contained a grid that would pass all the grains smaller than 1000 μm through the sieve. As a result, debris, for examples shells and twigs, were not included into the grain size distribution. The 10 remaining sieves contained grids that prevented larger grains to be released into the next sieve. These 10 sieves had the following grain size classes; 850 – 1000 μm , 710 – 850 μm , 600 – 710 μm , 500 – 600 μm , 425 – 500 μm , 300 – 425 μm , 250 – 300 μm , 180 – 250 μm , 106 – 180 μm and 0 – 160 μm . By putting the sieves on a shaking device for 10 minutes, the sand was distributed over the 11 sieves (see Figure 9 A). By determining the weight of each sieve on an accurate scale before and after sieving (see Figure 9 B), the percentage of the total amount of measured sand was calculated, in which the weight of the first sieve was not included. As a result from the weight in the remaining sieves, a cumulative curve was made from fine sand (0 %) towards course sand (100 %), so the D_{10} , D_{50} and D_{90} were determined.

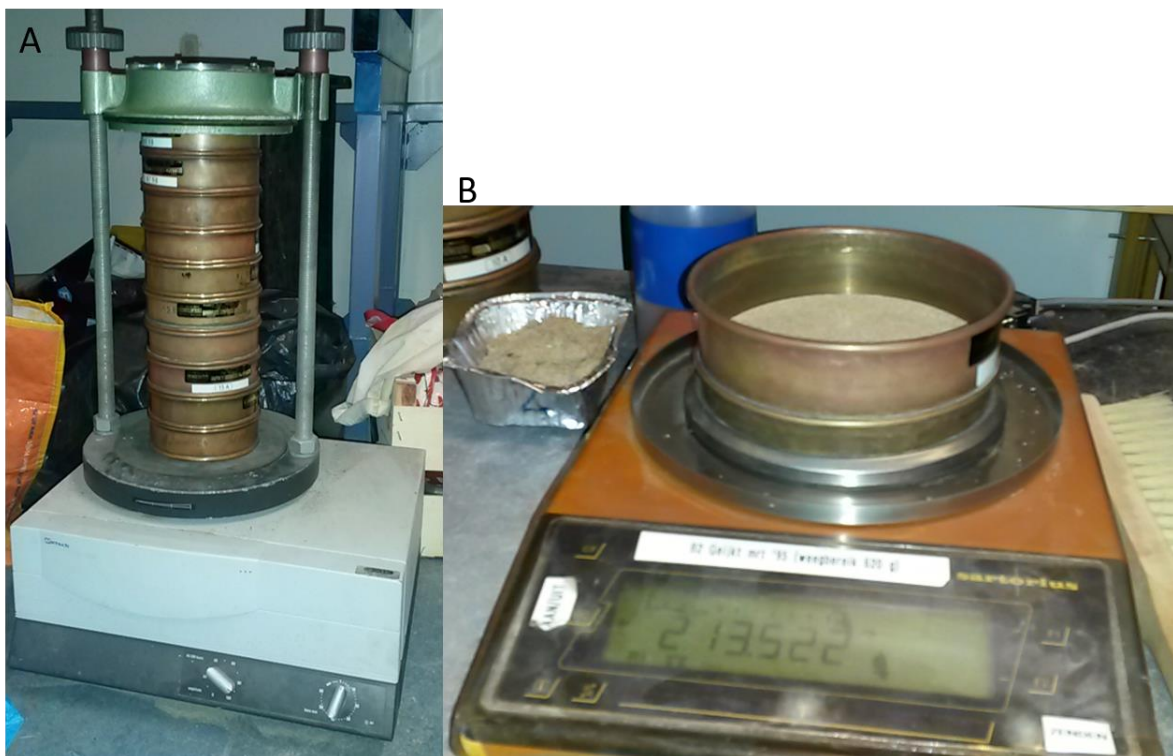


Figure 9: A; the 11 different sieves on top of each other at the shaking device. B; Scale where all the individual sieves are weighted on, before and after the sand samples are put into the sieves.

3.4 Data analysis

3.4.1 Start point of aeolian mass fluxes

The observed aeolian mass fluxes are plotted against the down-wind distance in section 4.1. For the longshore aeolian mass fluxes the starting point was always determined zero, because it was not possible to determine the upwind starting point of the fetch length. The starting point for the cross-shore aeolian mass fluxes is also determined zero, because it was too difficult to indicate the swash line during that measurement day. As a result, the MWAC sediment catchers can already measure aeolian mass fluxes at the starting point.

3.4.2 Linking wind speeds

To link the wind conditions, the corrected wind speed values are plotted in meteorological figures (section 3.5). As a result, a comparison can be made between the two measured wind conditions devices at the different locations at the beach during the same event.

In order to couple the different measured aeolian mass fluxes with the wind conditions. The mean values of the nearest sonic anemometer or cup anemometer were used during the same measurement period of the MWAC sediment catcher, so a mean wind speed and wind direction was determined for each aeolian mass flux location. As a result, a comparison was made between all the different measured aeolian mass fluxes and the wind climate (see section 4.2).

3.4.3 Grain size distribution

All the sand samples that were taken over the beach are combined with the sand samples that were taken in front of the MWAC sediment catchers. As a result, two grain size figures were made to give an indication of how the grain size varied over the beach through time. The first time period is from October 19 to October 24, and the second time period is from October 27 to October 29. A statistical analysis was determined for the two measurement periods and was done by calculating the inverse distance weighting (IDW) between the measurements points (see Appendix). From these two analysis a change through time for the whole field site is made and is further explained in section 4.3.3.

3.5 Measurement locations and meteorological conditions

During the two field campaigns, five days have been picked to represent the best situations essential for this research. When aeolian sand transport was expected during the field campaigns, two aeolian measurement set-ups could be placed, consisting of an array with MWAC sediment catchers, which were placed at various locations over the beach as is shown in Table 1.

Table 1: Overview of the different arrays and their locations on the beach, the direction of positioning and the maximum of sediment catchers than could be placed during the fieldwork campaigns.

MWAC sediment catchers			
Location of the array	Dune foot	Intertidal and/or upper beach	
Direction of the array	Longshore	Cross-shore	Longshore
Maximum of sediment catchers that could be used	7	10	10

The first array was located at the dune foot and was always positioned in longshore direction, so an indication of the amount of aeolian sand transport was made along the dune foot (see Figure 11 A to Figure 14 A). The second array could be placed at the intertidal and/or at the upper beach, which had the result that aeolian sand transports were measured in the main wind direction, and could give an indication about how aeolian sand flux was build up over the beach. The position of the array could vary from longshore to cross-shore (see Figure 10 A, Figure 11 A, Figure 13 A and Figure 14 A). During each measurement day the two arrays could be repositioned, which was dependent on the main wind direction.

For each measurement day, overviews of the different arrays that are used are shown in Table 2. Table 2 also contains information about the average weather conditions measured at the beach (see Figure 10 B to Figure 14 B). Table 3 shows the hourly average weather conditions measured 10 m above the ground at the nearby weather station, de Kooy, Den Helder (Figure 5).

Table 2: An overview of the 5 measurement days, the MWAC sediment catchers and their locations, the mean wind speeds and the mean wind directions.

	Measurement day							
	April 2	October 7		October 21	October 22		October 24	
Location of the MWAC sediment catchers	7 at the intertidal and the upper beach area	5 at the upper beach area	7 at the dune foot	5 at the dune foot	8 at the intertidal and the upper beach area	7 at the dune foot	5 at the upper beach area	5 at the dune foot area
Mean wind direction (°)	350	185 – 190	190 – 195	175 – 185	285 – 295	265 – 275	185 – 195	185 – 190
Mean wind speed (m/s)	6 – 7.5	6.5 – 7.5	6 – 7	5.5 – 9	5 – 7.5	4 – 5.5	5 – 7	5 – 6.5
Figure with the overview of the measurement locations and conditions	11	12		13	14		15	

Table 3: An overview of the measured hourly average wind speeds and wind conditions at de Kooy, Den Helder during the measurements at the study site.

April 2			October 7			October 21		
Measured hour	Hourly average wind direction (°)	Hourly average wind speed (m/s)	Measured hour	Hourly average wind direction (°)	Hourly average wind speed (m/s)	Measured hour	Hourly average wind direction (°)	Hourly average wind speed (m/s)
11	320	9	11	180	6	11	230	7
12	320	9	12	180	7	12	220	8
13	330	9	13	190	7	13	240	9
14	320	9	14	190	7	14	230	9
			15	200	9			
			16	200	8			
			17	210	7			

October 22					October 24				
Measured hour	Hourly wind direction (°)	average wind speed (m/s)	Hourly wind speed (m/s)	average wind speed (m/s)	Measured hour	Hourly wind direction (°)	average wind speed (m/s)	Hourly wind speed (m/s)	average wind speed (m/s)
14	280		8		13	190		6	
15	280		8		14	200		7	
16	280		8		15	210		7	
17	280		7		16	210		7	
18	280		7		17	210		6	
19	290		6						

In order to get a better overview of the starting and ending time between the two arrays, there is made a division between longshore and cross-shore runs in the metrological figures (see Figure 10 B to Figure 14 B), as was also done in Table 2. The dune foot array runs are indicated with vertical black dotted lines, while the intertidal and upper beach runs are indicated with vertical black solid lines. Furthermore, two beach poles that were located in the field site are incorporated into the figures of the area, in order to couple all the measurement locations with one another.

In Table 2 and Table 3 an overview of the mean wind speed and direction is given for the whole measurement day. The actual measured wind at the beach is shown in Figure 10 B to Figure 14 B, and in these figures a large variability in wind speed can be noticed during the measurement days. Therefore, the wind conditions measured at the beach and gathered from the nearby weather station will be discussed for each used measurement day.

At April 2nd, the wind speed was varying from 5.5 – 8 m/s. The correctness of the wind speed may be discussed, because the cup anemometers measured not continuous through the day and wind direction was not measured. The measured wind speeds and directions were compared to the

nearby weather station and equal wind speed measurements were observed. However, the wind direction was different than observed at the field (see Table 1 and Figure 10).

In Figure 11 B it was observed that at the start of the first measurements the wind speed was highly variable and changed from 4 – 7.5 m/s and during the same time the wind direction was also variable. While after 12 o'clock, the wind speed and direction became more constant and decreases during the measurement time. A variation in wind direction between the two measurement locations was noticed around 14:30. Around this time the wind direction at the beach changed to longshore, while the wind direction at the dune foot remained the same. It was also noticed that the wind measurements at the dune foot were lower than at the upper beach after 12:15. Comparing the wind data from the nearby weather station with the measured wind data at the field site, it was noticed that at the end of the measurement day, after 15 o'clock, the wind speed increases at the weather station. While at the field site, a decrease in wind speed was measured. The same observation was made for the wind direction for both locations (see Table 3 and Figure 11 B).

At October 21st, there was much variation noticed between the wind speed measurements at the beach. Before 12:30, a negative correlation was noticed between the wind speed measurements at the dune foot and at the intertidal and upper beach. At the moment the wind speed increases at the dune foot, the wind speed decreases at the intertidal and upper beach and vice versa. After 12:30 the wind speed for all measurement devices increases till the end of the measurement day from 6 – 7 m/s to 7.5 – 9 m/s (Figure 12 B). Comparing the wind data from the nearby weather station with the measured wind data, the same increasing trend in wind speed was noticed. However, the measured wind direction was not equal for both measurement locations (Figure 12 B and Table 3).

In Figure 13 B again a high variation in the wind speed measurements was noticed over the beach. The lowest wind speed measurements were measured at the dune foot and the highest wind speed measurements over the beach were done at the intertidal beach. This indicates that the wind speed decreases from the water line towards the dune foot. A variation in wind direction was also observed between the intertidal beach and the dune foot, since the wind direction at the dune foot was onshore and the wind direction at the intertidal beach was slightly oblique (west-northwest). The highest wind speed measurements were done at the dune trough, which was positioned in the dunes (see Figure 13). The same decrease in wind speed at the end of the measurement day was also observed at the nearby weather station (see Table 3).

At October 24th, again a negative correlation was noticed between the wind speed measurements at the dune foot and at the upper beach before 15 o'clock (Figure 14 B). The wind speed at the upper beach increased from the start of the measurements until 15 o'clock, while the wind speed at the dune foot exactly applies the opposite. At both measurement locations, the wind changed towards more longshore direction. However, a delay in the change in wind direction can be

observed between those two measurement locations. The wind data measured at the nearby weather station indicates a slightly higher wind speed than measured at the field site and the wind direction was again different between the nearby weather station and the field site (see Figure 14 B and Table 3).

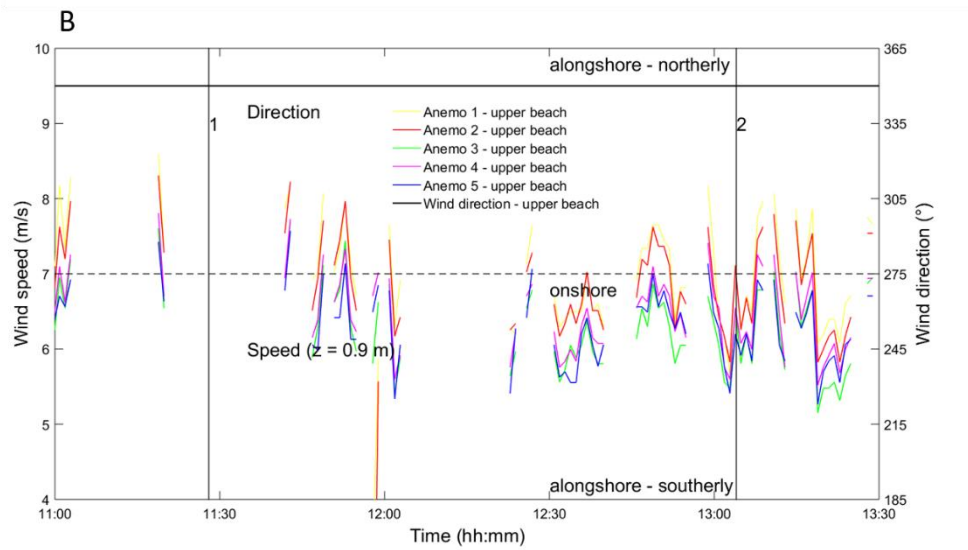
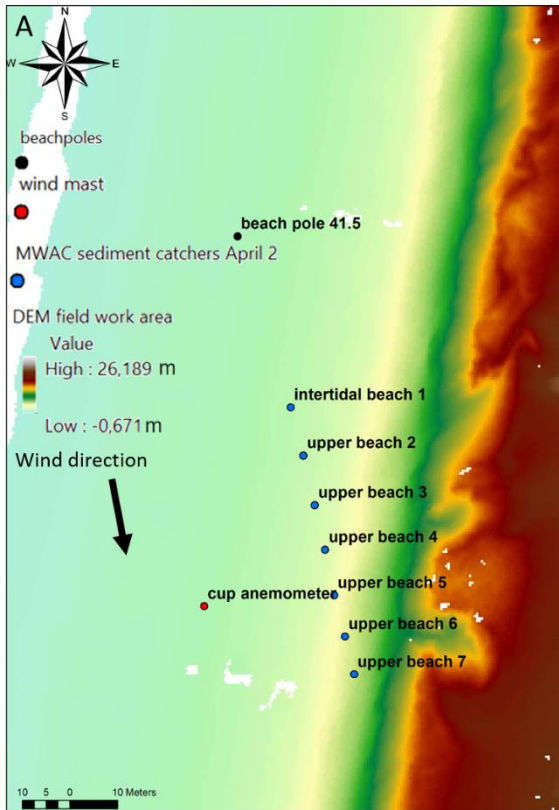


Figure 10: A; the locations of the different measurements at April 2. B; the wind speeds (colour lines) and wind directions (black line) for one locations. The vertical solid lines 1 and 2 indicate the starting and ending time of the run that is done at the intertidal and upper beach array during the event.

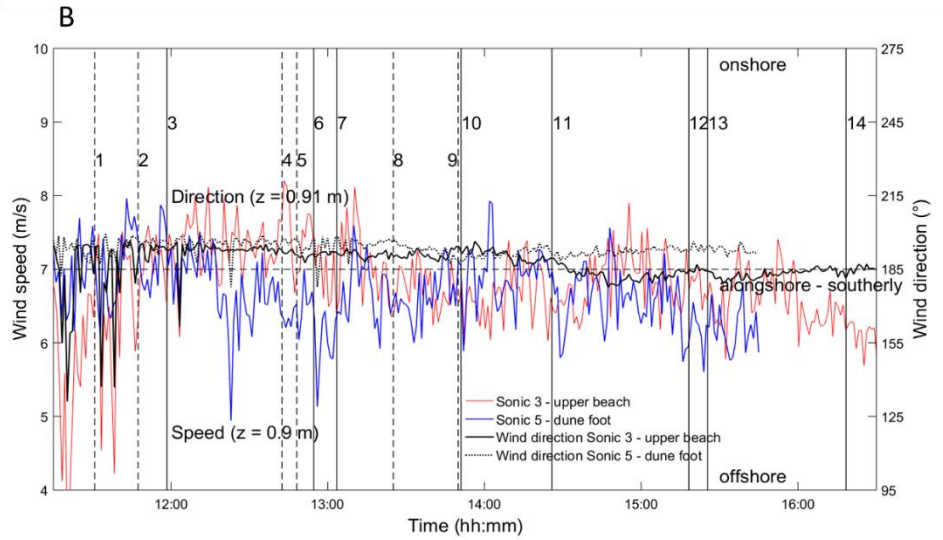
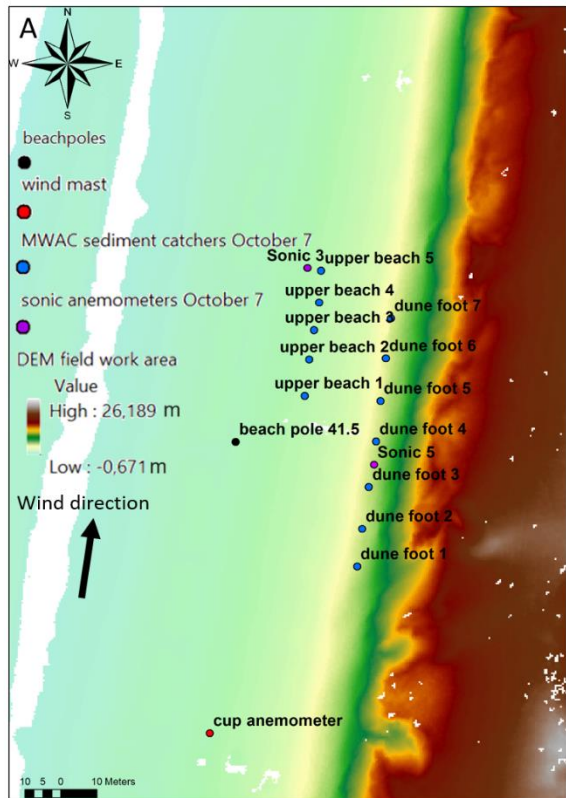


Figure 11: A; the locations of the different measurements at October 7. B; the wind speeds (colour lines) and wind directions (black lines) for different locations. The vertical lines indicate the start or end time of the different runs that are done during the event. The dotted lines indicate the measurements at the dune foot, while the solid lines indicate the measurements at the upper beach. The numbers 1, 2 and 4 indicate the start of the measurements at the dune foot, while the numbers 5, 8 and 9 indicate the end of the measurements at the dune foot. The numbers 3, 6, 11 and 12 indicate the start of the measurements at the upper beach, whereas the numbers 7, 10, 13 and 14 indicate the end of the measurements at the dune foot.

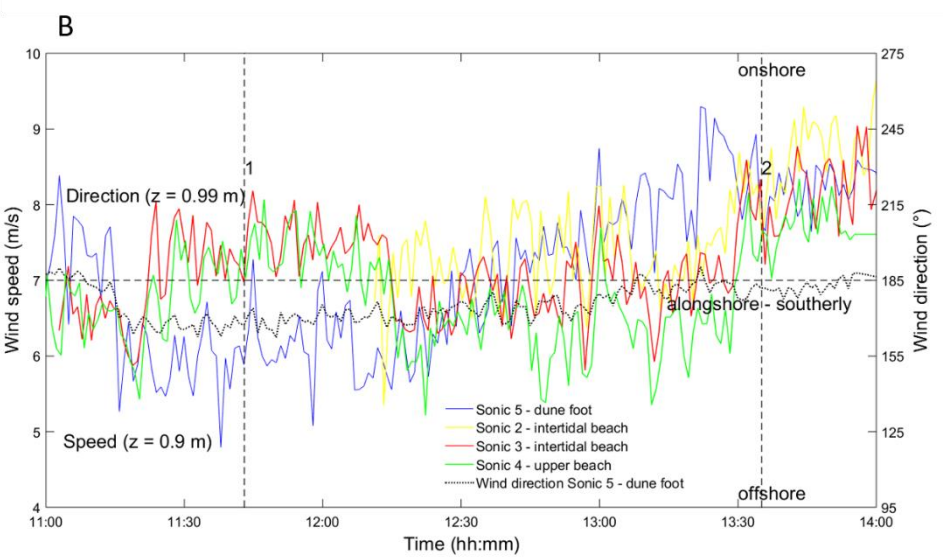
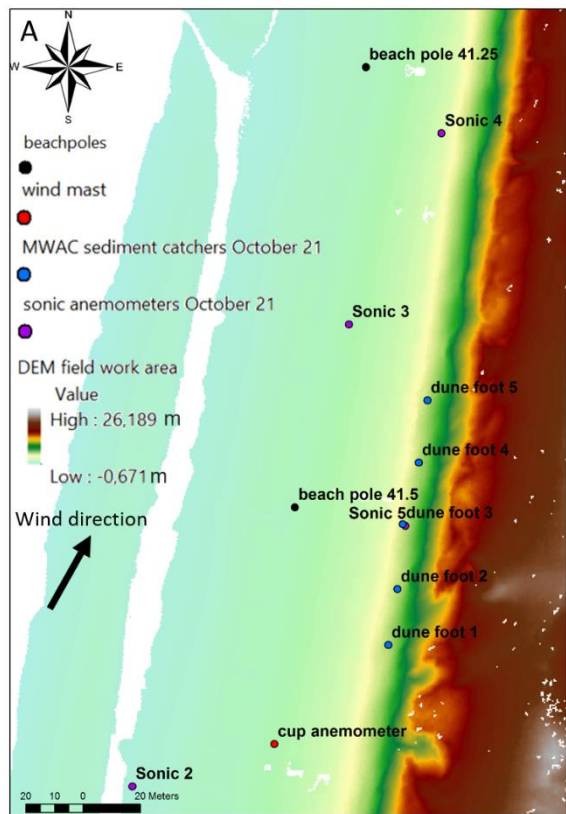


Figure 12: A; the locations of the different measurements at October 21. B; the wind speeds (colour lines) and wind directions (black line) for different locations. The vertical dotted lines 1 and 2 indicate the starting and ending time of the run that is done at the dune foot during the event.

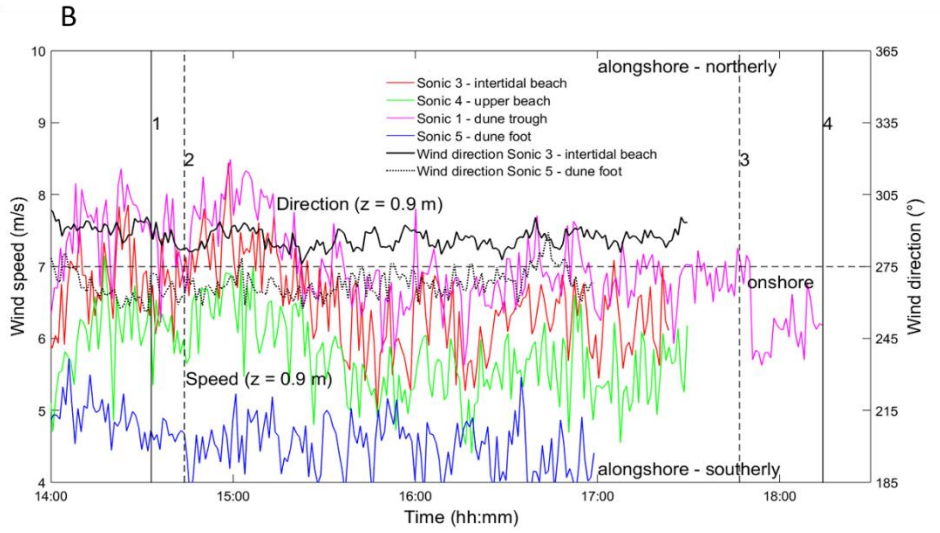
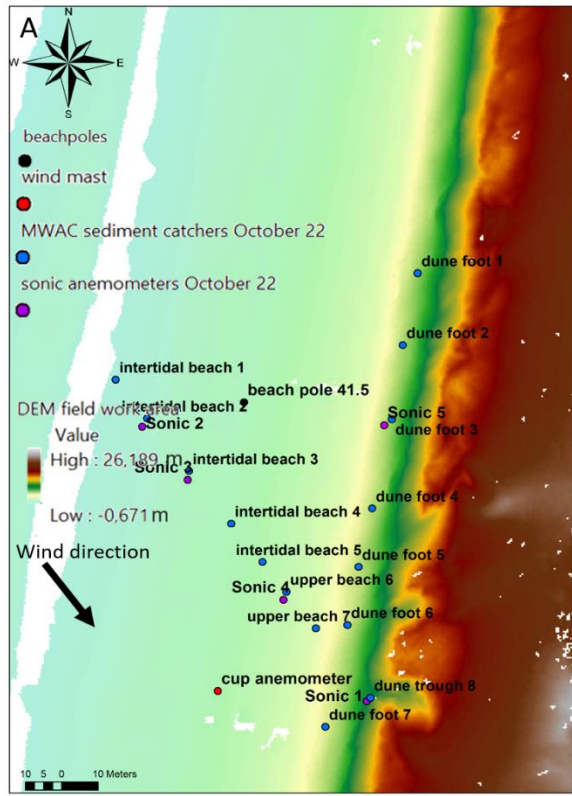


Figure 13: A; the locations of the different measurements at October 22. B; the wind speeds (colour lines) and wind directions (black lines) for different locations. The vertical lines indicate the start or end time of the different runs that are done during the event. The dotted lines indicate the measurements at the dune foot, while the solid lines indicate the measurements at the intertidal and upper beach. The numbers 2 and 4 indicate the start and end of the measurements at the dune foot, while the numbers 1 and 3 indicate the start and end of the measurements at the intertidal and upper beach.

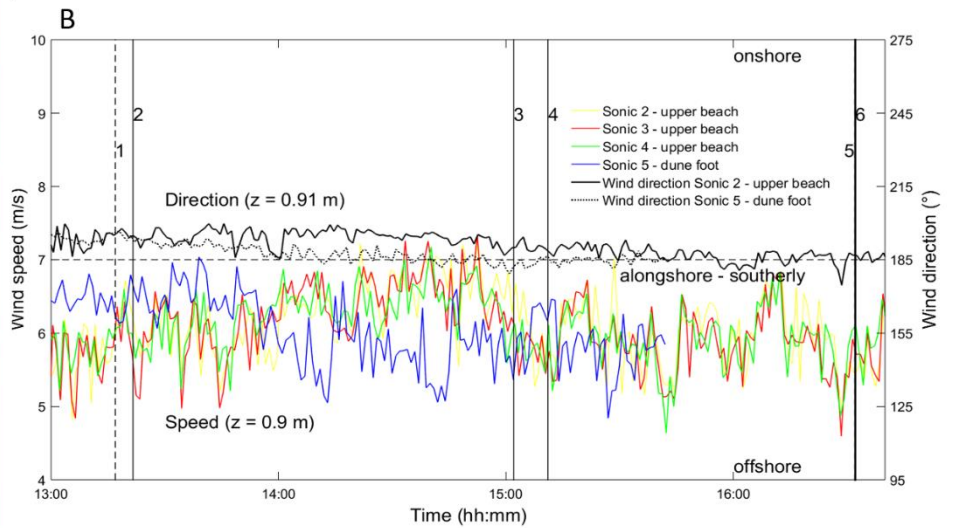
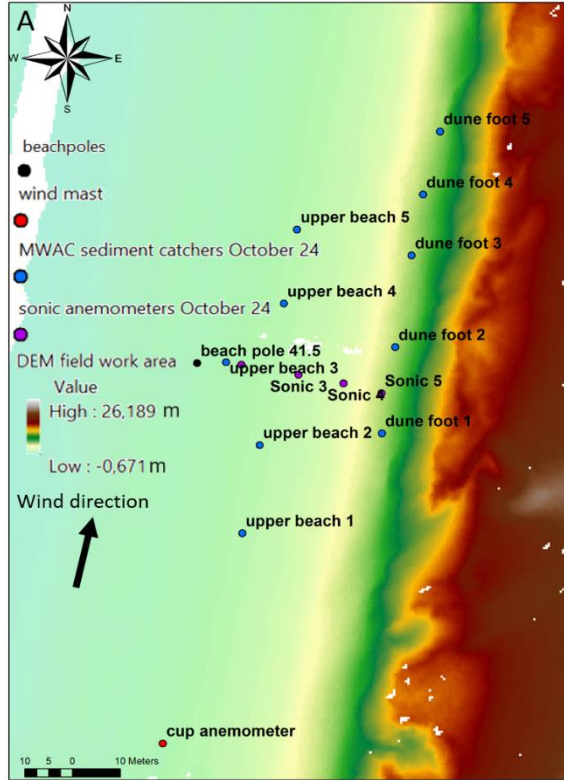


Figure 14: A; the locations of the different measurements at October 24. B; the wind speeds (colour lines) and wind directions (black lines) for different locations. The vertical lines indicate the start or end time of the different runs that are done during the event. The dotted lines indicate the measurements at the dune foot, while the solid lines indicate the measurements at the intertidal and upper beach. The numbers 1 and 5 indicate the start and end of the measurements at the dune foot. The numbers 2 and 3 indicate the start of the measurements at the intertidal and upper beach, while the numbers 4 and 6 indicate the end of the measurements at the intertidal and upper beach.

4. Results

4.1 Fetch length and aeolian sand transport

4.1.1 Cross-shore fetch conditions

During cross-shore measurement conditions aeolian mass flux was limited by the swash line and can start to increase after it passed the water line (section 2.2). Figure 15 shows that during all the cross-shore measurement conditions (2 events) the same increase in aeolian mass flux was observed with increasing fetch distance. However, the amount of aeolian mass flux transported in down-wind direction varies between both measurement days. A decrease in aeolian mass flux was noticed for the last two measurement locations on April 2, while this decrease was not noticed in the measurements on October 22. The measurements on April 2nd indicate that the critical fetch was already exceeded more upwind of the sediment catchers. The measurements on October 22nd indicate that this critical fetch location was after the 4th sediment catcher. Comparing the locations of the both measurement days, the location of the first sediment catcher on April 2nd, was at equal distance from the dunes in comparison to the 5th sediment catcher, which was positioned at the end of the intertidal beach (see Figure 10 A and Figure 13 A). This may indicate that during the measurement event on April 2nd, the wind conditions were more favourable than during the measurement event on October 22nd. Or that the surface characteristics were more favourable during the measurement event on April 2nd. The amount of aeolian mass flux measured during the event of October 22 was below $0.005 \text{ kg m}^{-2} \text{ s}^{-1}$ and therefore the observed values might not be significant enough to be used for down-wind fetch relations over the beach.

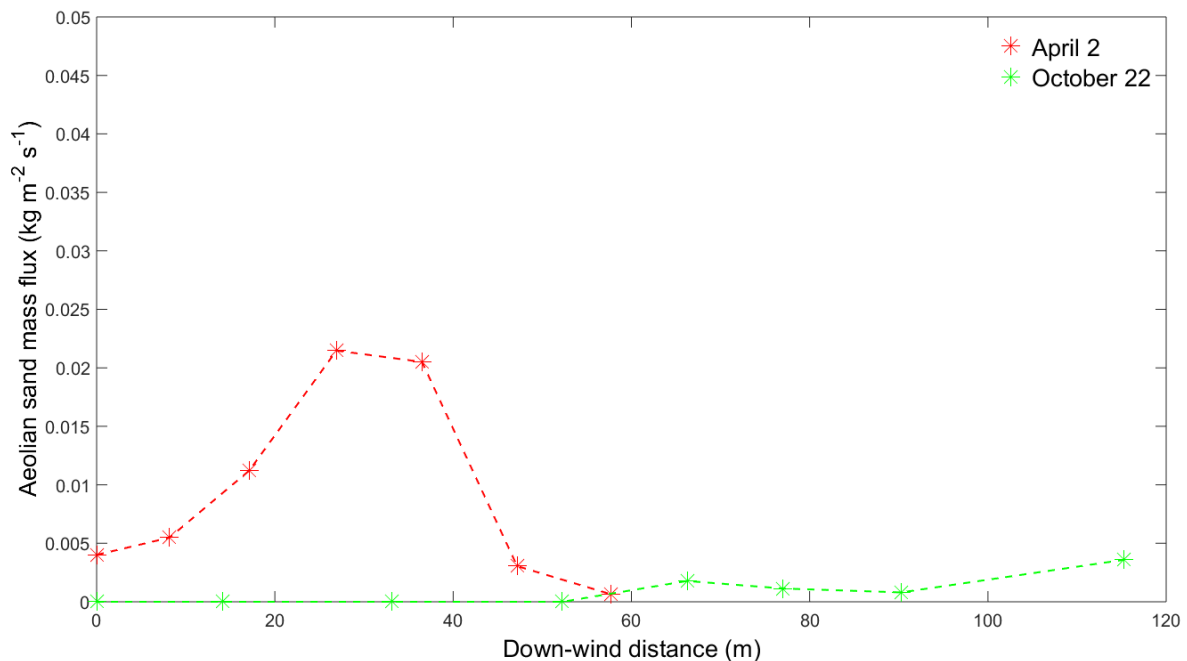


Figure 15: All aeolian mass flux measurements that were done in cross-shore direction over the beach during 2 events. For the measurement arrays, see Figure 10 A and Figure 13 A.

4.1.2 Longshore fetch conditions

During longshore measurement conditions the maximum fetch length was measured, because the upwind wind path was endless. Therefore, the expectation was that the maximum aeolian mass flux was measured in down-wind distance (section 2.2). However, comparing the measured longshore aeolian mass fluxes in Figure 16, the maximum aeolian mass fluxes were not observed during all the events. A clear difference was noticed between the longshore measurements at the dune foot (see Figure 16 A) and the longshore measurements at the upper beach (see Figure 16 B). Aeolian mass fluxes measured at the dune foot, might indicate that there was indeed a maximum fetch, which results in equal aeolian mass fluxes in down-wind direction during the same event. While this same equal trend was not observed at the upper beach. At the upper beach, aeolian mass flux remains increasing in down-wind distance. This would indicate that there was no maximum fetch length at the upper beach as would be expected with infinite fetch length.

There were two events, on October 7th and on October 24th, where measurements were done in longshore direction at the dune foot and at the upper beach at the same time (Figure 16). Due to the equal longshore direction and the equal fetch length, it was expected that aeolian mass fluxes in down-wind direction were equal for both arrays. However as described before, this equal aeolian mass flux pattern was not observed for both measurement arrays and the equal order of aeolian mass flux was also not observed between both measurement arrays. During the event on October 24th almost no aeolian mass fluxes were measured at the upper beach, while at the dune a significant large amount of aeolian mass flux was measured. While on October 7th a significant smaller amount of aeolian mass flux was measured at the dune foot than measured at the upper beach. These observations may indicate that there were different wind conditions or surface characteristics between the upper beach and the dune foot areas, which resulted in a delay for the increasing trend of aeolian mass flux over the upper beach.

Comparing the variations between the longshore aeolian mass fluxes measured at the dune foot, there were again some fluctuations within the down-wind wind path between $0.005 - 0.01 \text{ kg m}^{-2} \text{ s}^{-1}$. This same amount applies for the measurements at the upper beach in down-wind wind path during relatively normal amounts of fluxes. Therefore, it was expected that the general trend observed in Figure 16 is correct. However, when aeolian mass fluxes were below $0.005 \text{ kg m}^{-2} \text{ s}^{-1}$, it might be that the measured fluxes were too low and therefore not significant enough to use for down-wind fetch relations over the beach. This applies for the measurements that were done at the dune foot on October 22, and the measurements that were done at the upper beach on October 24.

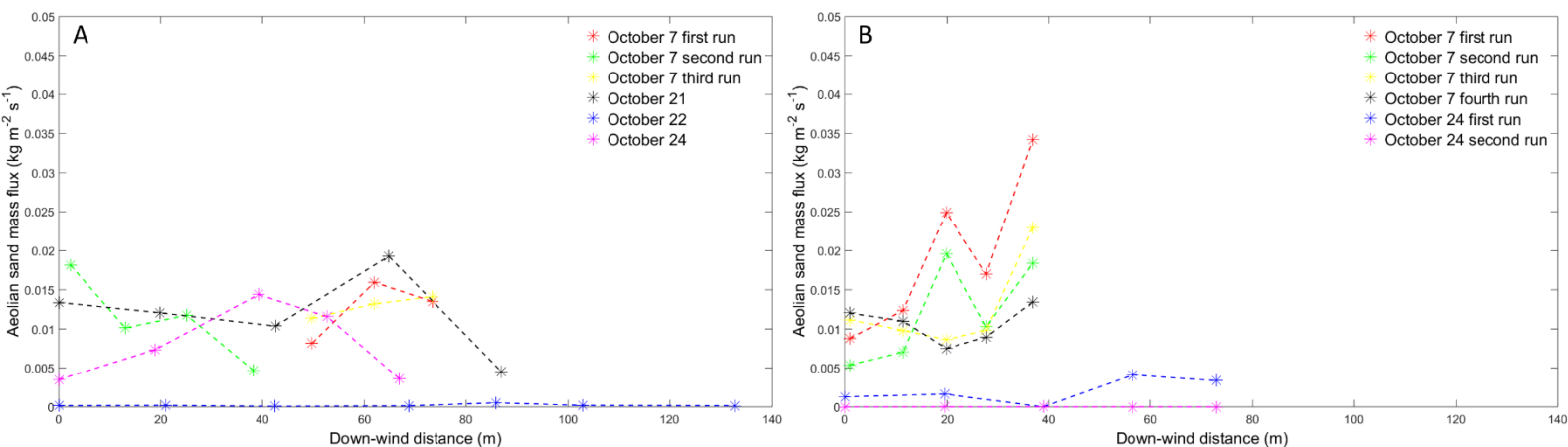


Figure 16: All aeolian mass flux measurements that were done in longshore direction over the beach. A; all aeolian mass fluxes measured at the dune foot during 4 events. B; all aeolian mass fluxes measured at the upper beach during 2 events. For the measurement arrays, see Figure 11 A to Figure 14 A.

4.2 Varying wind climate conditions

In order to find out how the different wind conditions affect aeolian mass flux in down-wind distance, first the longshore and cross-shore wind speed influences will be investigated. Second, the wind direction during the measurements is included and investigated.

4.2.1 Wind speed

In Figure 17 all the measured aeolian mass fluxes with their corresponding wind conditions are plotted. To measure aeolian sand transport the wind speed must exceed the critical shear stress before sand particles can be brought into motion (section 2.1). In Figure 17 it is shown that during the field campaigns the first measurements of aeolian mass flux occurred around a mean wind speeds of 5.8 – 6 m/s, and the highest mean wind speed was never larger than 7.5 m/s.

Comparing the cross-shore and the longshore aeolian mass fluxes with one another, a variation in aeolian mass flux and wind speed can be found (Figure 17). The cross-shore measurements of aeolian mass fluxes and the wind speeds at the intertidal and upper beach were relatively lower than during the longshore measurement at the upper beach and at the dune foot. Since there were only a few cross-shore measurements done during the field campaigns, no good correlation was made between the different parts of the beach based on the mean wind speed measurements. In general, it was observed that with increasing wind speed there was also an increase in aeolian mass flux. However, no clear relation was found when relations were plotted between the wind speeds and aeolian mass fluxes of; all the measured data points measured over the beach, the individual longshore measurements or the individual cross-shore measurements.

Comparing the mean wind speed of the sediment catchers with the measurements of one minute mean wind speeds during the same run at the different parts of the beach. It can be observed

that during all the events there was a high fluctuation in the one minute mean wind speed (see Figure 10 B to Figure 14 B), which might result in a decrease of the strength of the fetch and may indicate that the fetch length has to start over again after each decrease in wind speed. However, since this fluctuation in wind speed is natural, it might be that this fluctuation is not significant for aeolian mass flux results.

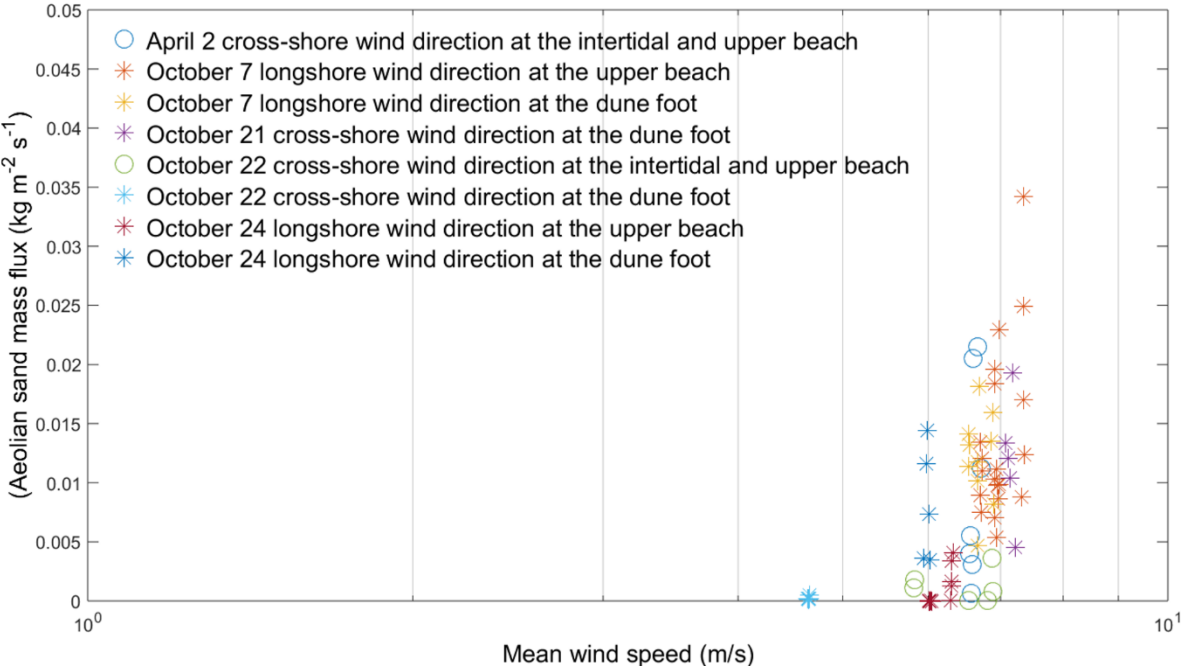


Figure 17: All the measured cross-shore and longshore wind conditions with their aeolian mass flux for each individual sediment catcher of the 5 events on a semi-logarithmic scale. A circle (O) means that the measurements were taken in cross-shore direction over the beach, while an asterisk (*) means that the measurements were done in longshore direction over the beach.

4.2.2 Wind direction

In order to find the influence of the wind direction on the down-wind aeolian sand transport, the wind direction was also incorporated in Figure 17. Comparing the influence of the cross-shore wind direction on aeolian mass flux. It was noticed that during the cross-shore wind direction an increase was observed in aeolian mass flux on April 2nd (Figure 15), while there was an equal wind speed of around 6.5 m/s for all the sediment catchers (Figure 17), which were positioned over the intertidal and upper beach. The variation in aeolian mass flux over the beach might indicate that at the intertidal beach, the fetch was not able to increase sufficient or that surface parameters might have had influence on aeolian mass flux. The decrease in aeolian mass flux measured at the end of the upper beach cannot be explained by the measurements done on April 2nd.

In Figure 15 also an increasing trend was found for aeolian mass flux measurements at the intertidal and upper beach on October 22nd. During this measurement day, the mean wind speed of the sediment catchers varied between 6 – 7 m/s (Figure 17). Even when some of the wind

measurements on October 22nd were higher than during the wind measurements on April 2, aeolian mass fluxes measured during that day were lower (Figure 17). This probably can be explained by the observation that during the measurement on October 22, the wind direction was more oblique than on April 2nd, with the consequence that the maximum fetch length was smaller on October 22. On October 22nd there were also aeolian mass fluxes measured at the dune foot, however almost no aeolian mass fluxes were measured during that day at the dune foot (Figure 16). This probably can be explained by the relatively low wind speeds around the 4.6 m/s, which were below the critical shear velocity and therefore the wind speed was probably not able to keep aeolian sand into motion.

During the cross-shore wind conditions measured at the dune foot on October 21, the measured wind speed was around 7.2 m/s for all of the sediment catcher locations (Figure 17). However no equal aeolian mass fluxes were observed in down-wind direction (Figure 16), which was not a logical consequence because the fetch length was equal for every sediment catcher. This might indicate that the upwind beach surface, i.e. the intertidal and the upper beach area, might have had varying surface parameters.

In Figure 17 also the longshore wind directions are included. This longshore wind direction ensures that the fetch can become infinite in down-wind distance (section 2.2). The influence of the longshore wind direction on aeolian mass flux was investigated. It can be noticed that on October 7 relatively large aeolian mass fluxes were measured for both measurement arrays. However, differences were detected between the upper beach measurements and the dune foot measurements. At the upper beach, the range of aeolian mass flux was relatively large and varied between $0.005 - 0.035 \text{ kg m}^{-2} \text{ s}^{-1}$. While the measured wind speeds also varied and were between $6.8 - 7.5 \text{ m/s}$, which was again relatively large. This large variation in wind speed was also noticed during the measurement day, where a decrease in the one minute mean wind speed was measured during the different runs (see Figure 11 B). This variation can probably be explained by the decrease of aeolian mass fluxes in down-wind distance which was observed in Figure 16. In the same figure, it is shown that the one minute wind direction also changed slightly $10 - 15$ degrees more towards the south at the upper beach (see Figure 11 B). This change in wind direction would probably favour the increase in aeolian mass flux. However, there was also a decrease in wind speed causing a decrease in aeolian mass flux. These two parameters give the combined result that aeolian mass flux had decreased from the first run towards the last run during the measurement day (Figure 16). In Figure 17 the same large variation in measured aeolian mass flux was observed at the dune foot, which was around $0.005 - 0.02 \text{ kg m}^{-2} \text{ s}^{-1}$. Nevertheless, the same large variation in wind speed was not observed and remained approximately equal for all the sediment catchers. Comparing aeolian mass flux variation in down-wind distance in Figure 16, it can be noticed that aeolian mass flux remained

approximately equal. Therefore, this variation in aeolian mass flux might be best explained by natural parameters of the beach.

On October 24 there were also longshore wind directions (Figure 17). Again there was a large variation observed between the different measurement locations over the beach. At the dune foot the wind speed was approximately equal for all the sediment catchers. However, aeolian mass flux varied between $0.005 - 0.015 \text{ kg m}^{-2} \text{ s}^{-1}$. When looking at the down-wind change in aeolian mass flux almost an equal down-wind pattern was observed, with only a decrease in aeolian mass flux at the end of the measurement array. Therefore, this variation in aeolian mass flux might be explained by a change in surface parameters in down-wind direction. However, when comparing the one minute mean wind speeds during the dune foot run (see Figure 14 B), it can be noticed that the wind speed was often below the critical shear velocity. This might indicate that at certain moments the wind was not strong enough to keep aeolian sand into motion. Therefore, the measured aeolian mass flux might not be representative for the entire run and only indicate aeolian mass fluxes that were raised in the gusts of the wind. In Figure 17 a clear change in aeolian mass flux and wind speed was observed at the upper beach. During the first run almost no aeolian mass fluxes were measured and varied between $0 - 0.005 \text{ kg m}^{-2} \text{ s}^{-1}$, while the wind speeds remained approximately the same. However, during the second run no aeolian mass fluxes were measured, even when the wind speeds were above the critical shear stress. The observed aeolian mass fluxes during the second run might best be explained by the decrease in the one minute mean wind speeds (see Figure 14 B). This ensures that the fetch has to start over again after each decrease in the wind speed. Secondly, the observed variation in aeolian mass fluxes might be explained by the upwind surface parameters, which could be more unfavourable. However this theory is unlikely, since the one minute mean wind direction became more favourable during the second run (see Figure 14 B).

Comparing all the longshore and cross-shore wind condition measurements with the measured aeolian mass fluxes, it can be noticed that at the moment the wind direction was longshore more aeolian sediment was measured. While during cross-shore measurements, it takes longer before aeolian mass flux increases. Even if the cross-shore wind speeds were approximately equal during the longshore wind speed measurements.

4.3 Morphology

In order to find out what the influence of morphology is on the down-wind aeolian mass flux at different parts of the beach, three different surface parameters will be discussed. First the influence of the beach profile will be discussed on the down-wind aeolian mass flux in combination with grain size variation and surface moisture content. Second, morphological parameters, i.e. grain size and

surface moisture content, and their influence on aeolian mass flux were compared with one another. Lastly, the varying beach profile will be looked at through time and how this might influence the down-wind aeolian mass flux.

4.3.1 Down-wind fetch relations

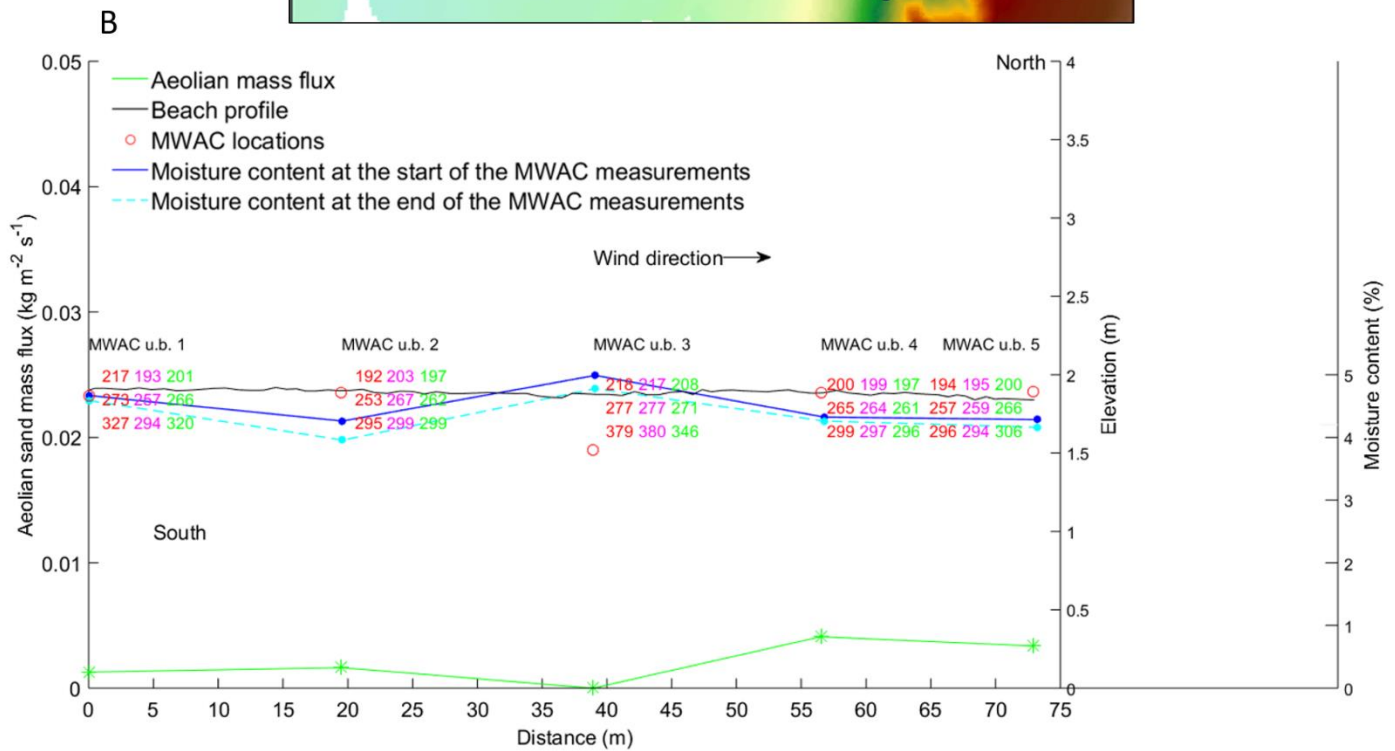
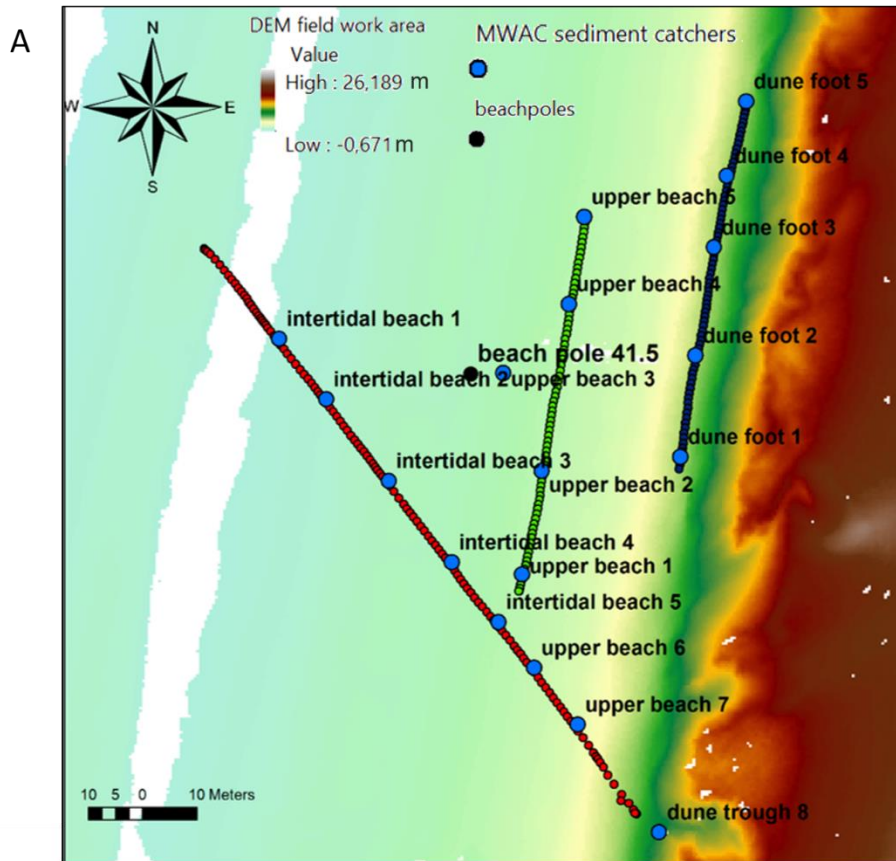
In order to find out what the influence of the morphology on the aeolian mass flux in down-wind distance at different parts of the beach is, three different morphological parameters and the measured aeolian mass fluxes are shown in Figure 18. Figure 18 A shows the three different measurement profiles that will be discussed, which represent the different parts of the beach. The first morphological profile was in longshore direction at the upper beach and was measured on October 24th (Figure 18 B). The second morphological profile was in longshore direction at the dune foot and was also measured on October 24th (Figure 18 C). The last morphological profile was in cross-shore direction and was measured at the intertidal beach, the upper beach and at the dune trough on October 22nd (Figure 18 D).

During the measurements at the upper beach array, the 3rd MWAC sediment catcher was located 1 meter more in seaward direction (see Figure 14 A). Therefore, the surface moisture content was around 1 % higher for that measurement location compared to the other locations along the array (Figure 18 B). At this measurement location two different runs were done, and for both runs the grain size and surface moisture content were measured before and after the run. The grain size variation remained approximately equal at the beach for each measurement location during the run, but the grain size varied slightly in down-wind direction between 5 – 10 μm over the beach. Comparing aeolian mass fluxes over the beach, it can be observed that lower aeolian mass fluxes were measured where the surface moisture content was higher. During the second run no aeolian mass fluxes were measured, while the surface moisture content had not changed (Figure 18 B). Therefore the observed change in aeolian mass flux can probably be explained by the decrease in wind speed, which declined to the critical shear velocity of 6 m/s, while the wind direction remained the same during both runs (see Figure 14 B).

During the measurements at the dune foot, the surface moisture content and the grain size remained the same during the run (Figure 18 C). Due to the small variations in these two morphological parameters, it is assumed that the grain size distribution and the surface moisture content had limiting influence on aeolian mass flux in down-wind direction. During the run the average wind speed was relatively low for aeolian sand transport to start, but the wind direction ensured a long fetch over the beach (see Figure 14). This long fetch was probably the major factor that favoured aeolian mass flux at the dune foot. The height of the beach varied slightly in down-wind direction, between 0.1 – 0.4 m, while the largest variation in height was observed between the

4th and 5th sediment catcher. At these two measurement locations a decrease in aeolian mass flux was observed in down-wind direction. This decrease in aeolian mass flux at the end cannot be explained by the fetch (Figure 18 C). Therefore it might be that a combination of the increase in beach height and a variation in wind direction has caused the decrease in aeolian mass flux.

During the measurements in cross-shore direction over the intertidal beach, the upper beach and the dune trough, it can be noticed that the first aeolian mass fluxes were measured at the moment the surface moisture content decreases (Figure 18 D). During the run, the largest decrease in surface moisture content was measured at the intertidal beach. Nevertheless at the end of the run, the surface moisture content was still too moist to bring sand particles into motion at the intertidal beach and the grain size changed in down-wind direction over the beach. At the intertidal beach, the grains were larger than at the upper beach and at the dune foot. But also a grain size variation can be observed at the intertidal beach before and after the run. At the bar, the grain size decreased for all grain size classes during the run (Figure 18 D). While in the trough all the grain size classes increased during the run. It remains difficult to determine the influence of these grain size variations on aeolian mass flux, because no sand transport was measured on this part of the beach. At the upper beach and at the dune foot, no large grain size variations were observed, but there was a large variation in height. Nonetheless, still an increase was observed in aeolian mass flux in down-wind direction (Figure 18 D). Therefore, the wind speed probably had the strongest influence on aeolian sand transport in down-wind direction and could only transport aeolian mass fluxes over the dry fetch segments (see section 2.3).



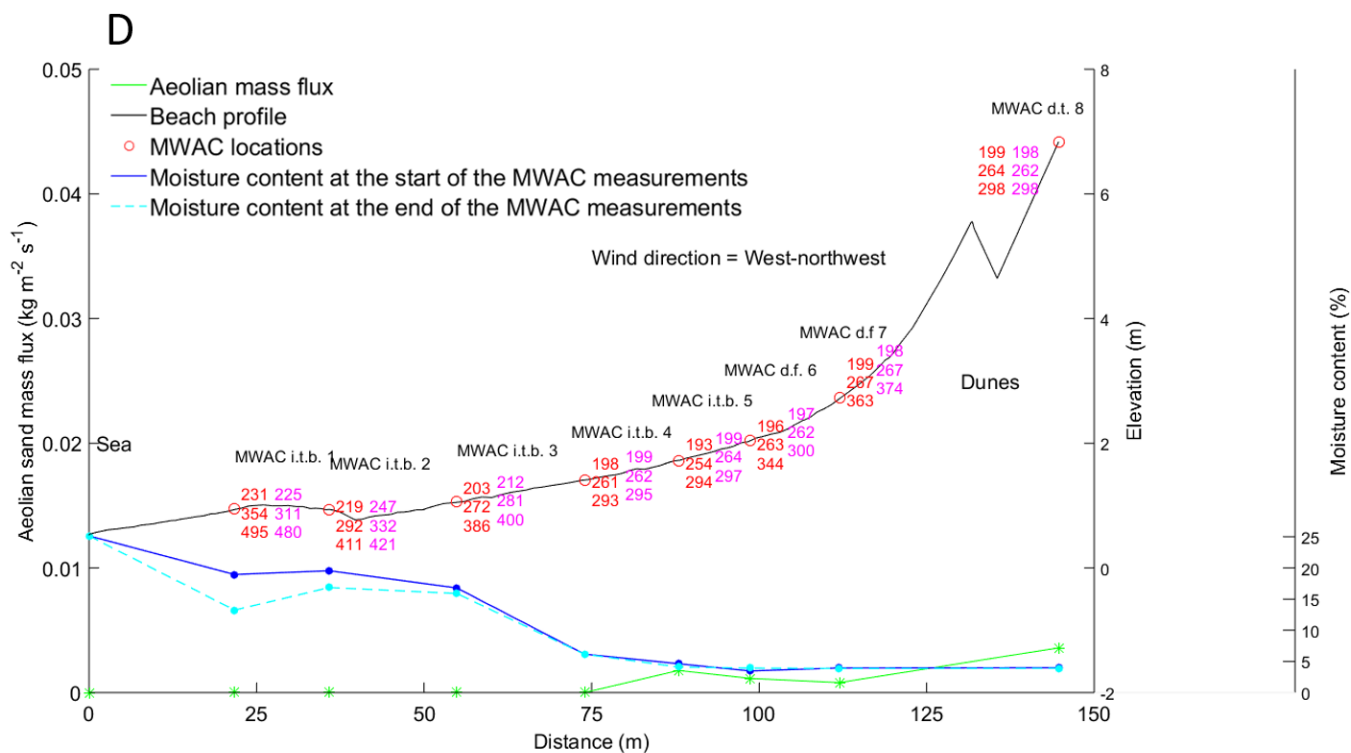
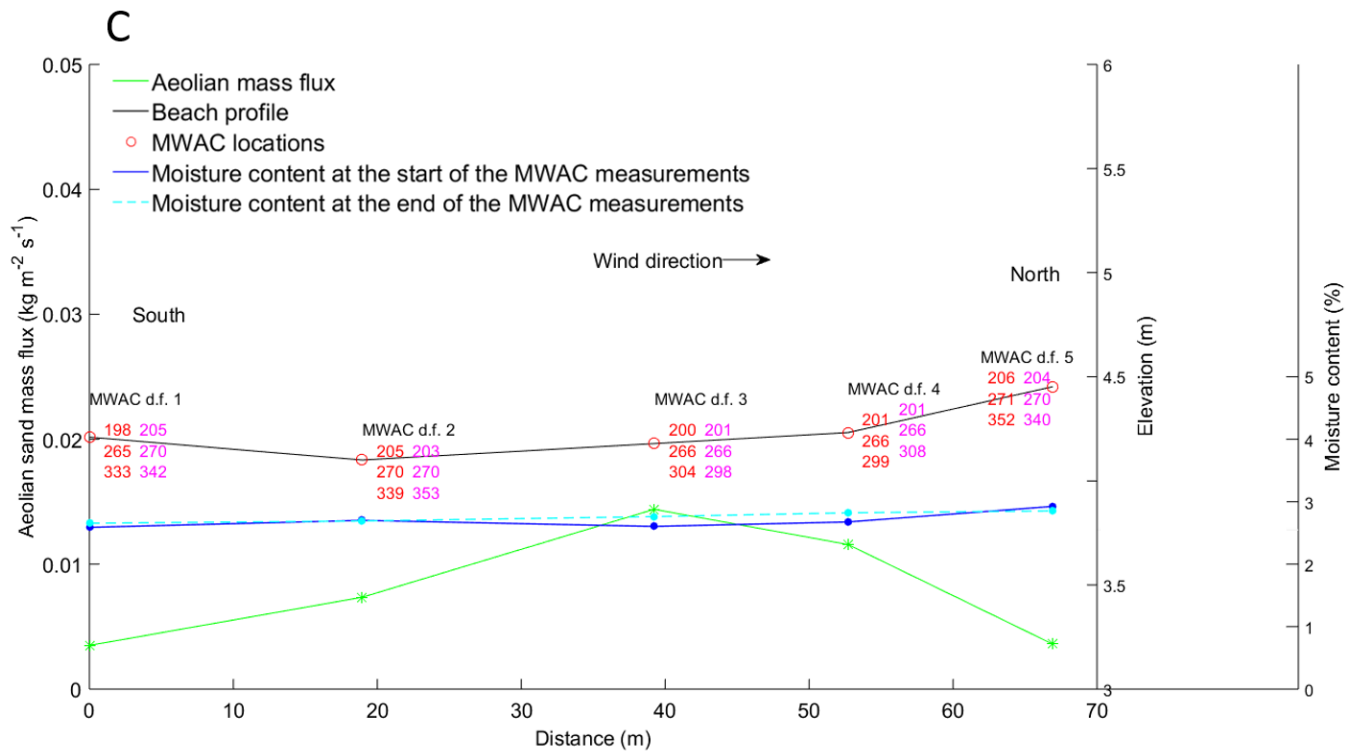


Figure 18: An overview of how aeolian mass fluxes (green line) react on different profiles over the beach with the three morphological parameters incorporated; the beach height, the surface moisture content and the grain size. The surface moisture content is measured before and after the run (dark blue = before, light blue = after) and also the grain size is measured before and after the run (red = before, pink = after). The grain size is divided in three different classes: top = D_{10} , middle = D_{50} , bottom = D_{90} . A; The three different measurement profiles that will be shown in more detail in Figure 18 B, C and D. B; Beach profile over the upper beach area in longshore direction. C; Beach profile at the dune foot area in longshore direction. D; Beach profile over the intertidal beach, the upper beach and the dune trough in cross-shore direction.

4.3.2 Morphological relations

In order to find out if there is a relation between aeolian mass flux and the surface parameters, these different factors were plotted against one another in Figure 19. In Figure 19 aeolian mass flux was plotted against two surface parameters: the mean grain size (D_{50}) (Figure 19 A) and the surface moisture content (Figure 19 B). The plotted aeolian mass fluxes are the same as used in section 4.3.1 and were plotted against the same values as used in Figure 18.

In Figure 19 A it is shown that higher aeolian mass fluxes are measured when the grains at the beach surface are relatively small and vary between 265 – 275 μm . These higher aeolian mass fluxes were mostly measured at the upper beach and at the dune foot area. It also can be noticed that aeolian mass fluxes were mostly measured during relatively low surface moisture contents, between 2 – 5 % (Figure 19 B), and higher aeolian mass fluxes were measured mostly at the upper beach and at the dune foot area. These observations from Figure 19 are in agreement with the down-wind observations as indicated in section 4.3.1. Figure 19 also shows that the measurements which were done in cross-shore direction at the intertidal beach, at the upper beach and at the dune trough, indicate that there was a higher grain size variation (250 – 350 μm) than that of the measurements which were done at the upper beach and dune foot area (250 – 280 μm).

In Figure 18 it is shown that the largest mean grain sizes were observed at the intertidal beach compared to the upper beach and the dune foot area for all profiles. This might indicate that larger wind speeds were needed to bring the sand particles into motion. Comparing the grain size for each measurement location before and after the run, it was noticed that the largest variations in grain size was measured during the measurements on October 22. During that measurement day, there was one measurement location that decreases strongly in mean grain size during the run, while there was one other location where the mean grain size increased during the run (Figure 19 A and Figure 18 D). However, no large variations in grain size were observed for the other measurements shown in Figure 19 A. Therefore the change observed during the measurements on October 22nd might indicate that there was some aeolian sand transport over the intertidal beach, probably in the form of creep, which resulted in a shift of grains at the measurement locations, because no aeolian sand transport was measured at this part of the beach (see section 2.1).

In Figure 19 B it can be noticed that the largest surface moisture contents were measured during the cross-shore measurements at the intertidal beach, which was also observed in Figure 18 D. This might indicate that both the surface moisture content and the grain size had influence on aeolian mass flux in down-wind distance. From Figure 19 it can be observed that during high grain size values also relatively large surface moisture contents were present. This same trend was previously noticed in section 4.3.1.

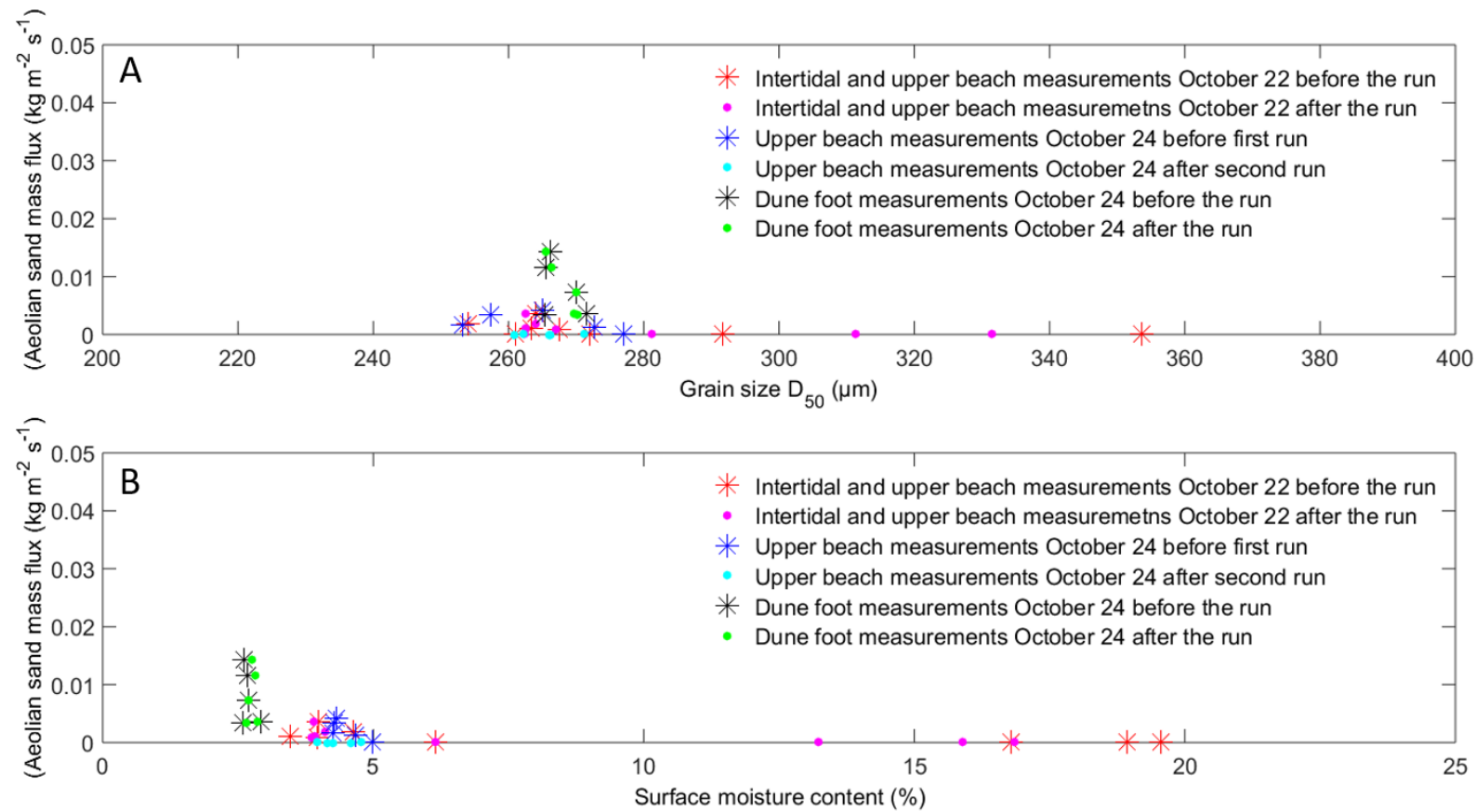


Figure 19: A; aeolian mass fluxes plotted against the mean grain size (D_{50}) for different measurements before and after a run was started. B; aeolian mass fluxes plotted against the surface moisture content for different measurements before and after a run was started.

4.3.3 Beach profile variation

The variation in the beach profile through time might have influence on the down-wind aeolian mass flux that will arise during aeolian transport events. In Figure 20 it can be noticed that the beach profile can change through time. In this figure the variation in time is shown between October 19 and October 28. During this time period, the bank and trough at the intertidal beach migrated towards the east, i.e. towards the dunes.

To find out what the influence might be of the variation in grain size through time on aeolian mass flux over the beach an overlay raster calculation was made, from the grain size measurements done between two time periods. The first time period was from October 19 till October 24 (see Appendix, Figure 22) and the second time period is from October 27 till October 29 (see Appendix, Figure 23). Whereupon, a comparison was made to give an indication how the grain size varies through time (Figure 21).

Comparing the grain size classes with one another, it was noticed that the overall grain size distribution over the beach becomes coarser through time. This change can especially be noticed for all the grain size classes in the west-southwestern corner of the field site (see Figure 21). In this area,

the D_{10} grain size class increases in general with $0 - 20 \mu\text{m}$, the D_{50} grain size class also increases but now with $20 - 40 \mu\text{m}$, while the D_{90} grain size class increases with $40 \mu\text{m}$ or more in this area. However, south-west of beach pole 41.5 a decrease in grain size can be noticed of $0 - 20 \mu\text{m}$ for the D_{10} and the D_{50} grain size class, while for the D_{90} grain size class in this area this decrease was not noticed that clear. The increase and decrease at the west-southwestern corner of the field site might be explained by that the bar and trough migrated more towards the east, which was also observed in Figure 20.

The expectation is that when the bar-trough system migrates more towards the dunes and that the grain size variation becomes in general coarser for all grain size classes, that this probably can have influence on aeolian sand transport in down-wind direction.

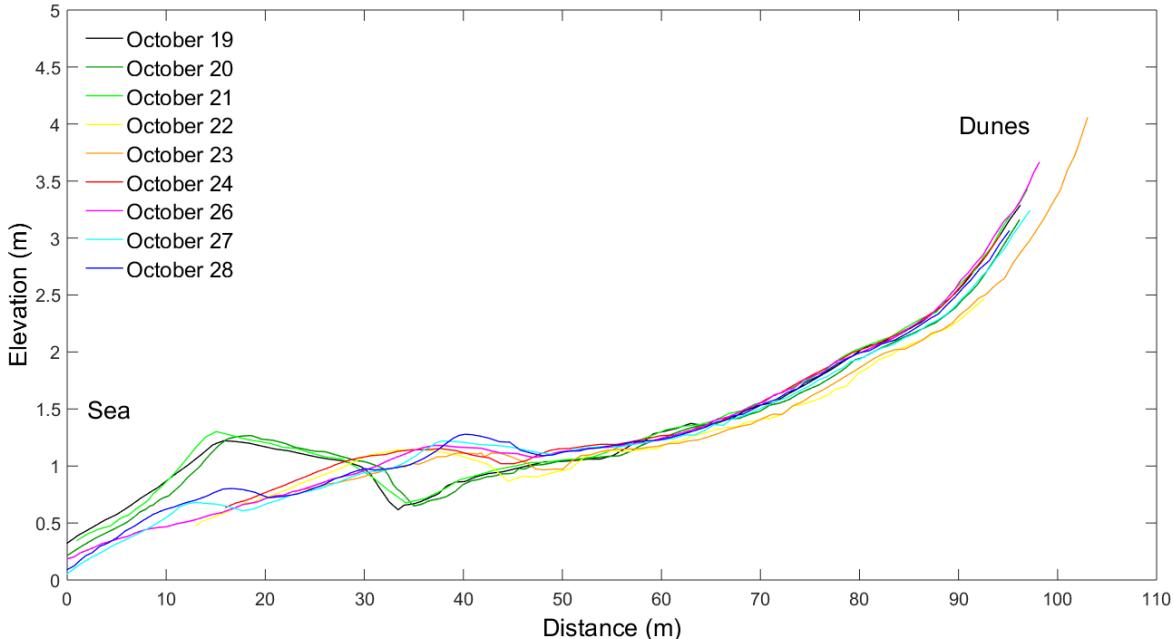


Figure 20: An overview of the change in beach profile through time for the different time periods used for the grain size distribution through time.

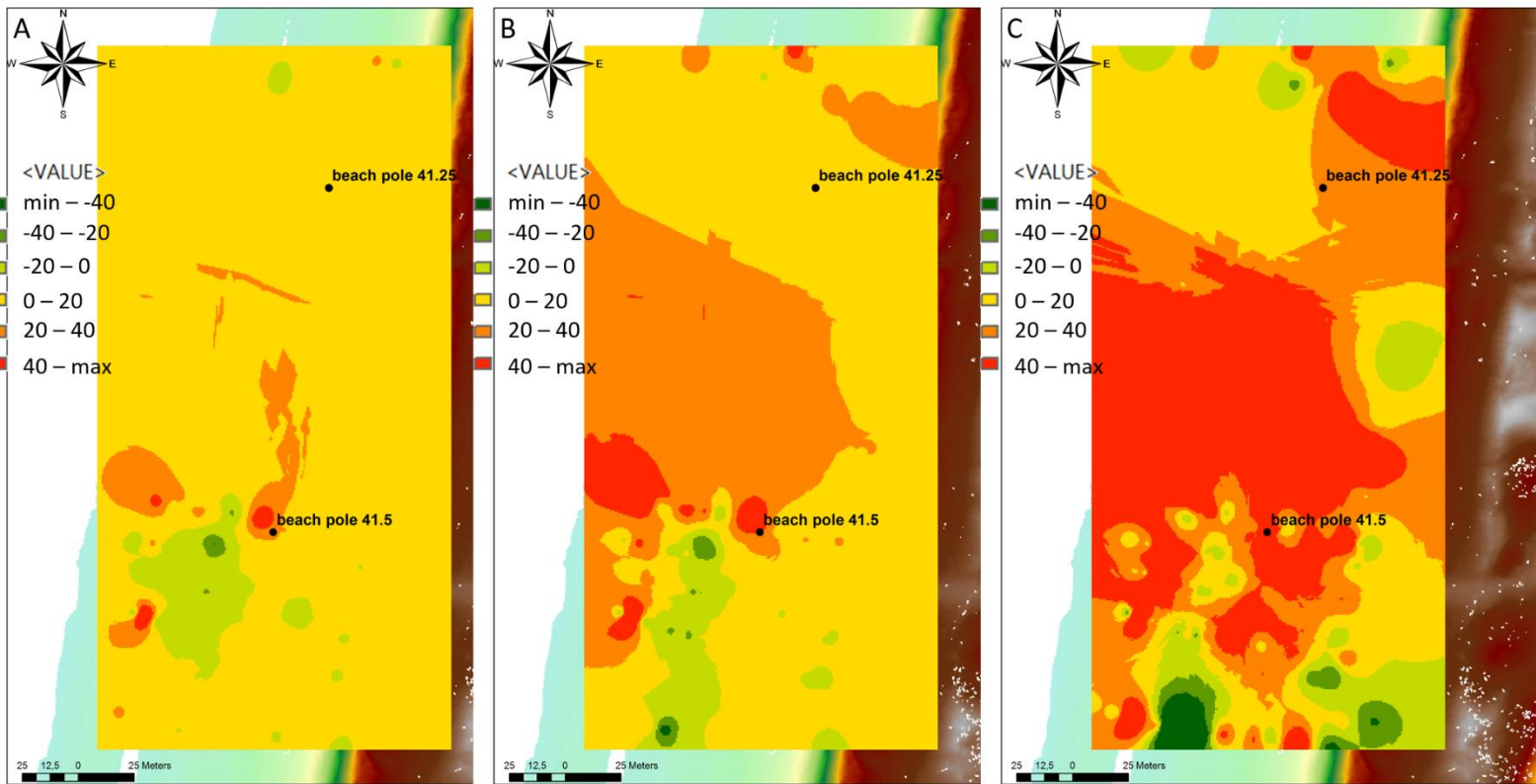


Figure 21: An overview of the grain size class variation through time, measurements were taken from October 19 to October 24 and from October 27 to October 29. A; the grain size variation through time for the D_{10} values. B; the grain size variation through time for the D_{50} values. C; the grain size variation through time for the D_{90} values. In the legend the variation values are in μm .

5. Discussion

The data obtained during the field work campaigns show that aeolian mass flux can be affected by multiple factors that will increase or limit aeolian sand transport in down-wind direction. The down-wind change in aeolian mass flux over a beach are still not yet fully explained in the literature (see section 2) and therefore the inputs in aeolian sand transport models are also still not entirely correct. The main observation made in the results is that each area of the beach is affected by different factors (see section 4). In the following paragraphs, the influence of the fetch length, the influence of the wind condition and the influence of morphology on aeolian mass flux are discussed. In order to give an indication about which factors have most influence at the different parts of the beach.

5.1 Influence of the fetch length

The down-wind aeolian mass flux data measured during this study can be compared with the down-wind aeolian mass flux findings done by Davidson-Arnott and Law (1990). When comparing both outcomes of the researches, it can be noticed that aeolian mass flux trends show a similar pattern in down-wind distance.

5.1.1 Cross-shore fetch length

For the intertidal beach and upper beach, it was noticed that during oblique measurement conditions aeolian mass flux increases in down-wind distance. These measurements were in agreement with the findings of Davidson-Arnott and Law (1990) as was expected in the hypothesis. The location of the start of aeolian mass flux was different for each event because the critical fetch was not equal during both measurement days. However, the same increasing trend can be observed in down-wind distance for both studies after aeolian sand transport has started, even when the critical fetch length was not equal (see Figure 3 and Figure 15).

During the cross-shore measurements on April 2nd, also a decrease in aeolian mass fluxes was noticed at the dune foot, which cannot be explained by the fetch theory presented by Bauer and Davidson-Arnott (2002) and Davidson-Arnott and Law (1990). While this same decreasing trend was not observed during aeolian mass flux measurements done on October 22. This finding might be explained by the low observed mass flux values during October 22. As a result of the low aeolian sand fluxes which were measured on October 22nd, a decreasing trend might not be noticed in down-wind distance. However, during the measurement day aeolian mass fluxes were below $0.005 \text{ kg m}^{-2} \text{ s}^{-1}$ and therefore the observed values might not be valid enough to use for down-wind fetch relations over the beach. But when there will be looked at the amount of sand that was captured over height in the different plastic bottles, which were used in the sediment catcher, the flux decreased in height

as was described by the theory of Ellis et al. (2009). Therefore the expectation is that even when aeolian mass flux is low, the measured fluxes below $0.005 \text{ kg m}^{-2} \text{ s}^{-1}$ on October 22 are valid. Comparing the measured aeolian mass fluxes with the measurements done by Davidson-Arnott and Law (1990), they also measured aeolian mass fluxes below the $0.005 \text{ kg m}^{-2} \text{ s}^{-1}$. As a consequence of the acceptance of these low flux values, the decrease in aeolian mass flux at the dune foot during the event on April 2 can still not be explained by only comparing the measured down-wind aeolian mass fluxes at the different measurement arrays.

5.1.2 Longshore fetch length

For the upper beach and dune foot area, it was noticed that during longshore measurement conditions aeolian mass flux varied in down-wind distance (see Figure 16). During the runs at the dune foot on October 7th, October 21st and October 24th (see Figure 16 A) it was shown that aeolian mass fluxes first increase in down-wind distance and at the end aeolian mass fluxes decrease again. This is not entirely in agreement with the expected aeolian mass flux patterns as predicted by the fetch theory presented by Bauer and Davidson-Arnott (2002) and Davidson-Arnott and Law (1990). These variations in mass flux might be explained by limiting parameters that influence aeolian mass flux in down-wind direction. During the runs at the upper beach on October 7th and October 24th (see Figure 16 B), an increasing trend was observed in down-wind distance. Which indicates that the maximum fetch length was not yet reached at the measurement array. This variation in down-wind distance was not observed during maximum fetch conditions in the research by Davidson-Arnott and Law (1990). In their research they assumed that at a certain down-wind distance, an equilibrium state in aeolian mass flux is reached (see Figure 3). Therefore the hypothesis is not correct because during longshore measurements the same equilibrium state will not be reached. The hypothesis made for the longshore measurements done during the same event at the upper beach and at the dune foot was also not correct. Because it was expected that the same measurement patterns would appear at the dune foot array and at the upper beach array. However, different aeolian mass flux patterns were measured during the same event at the upper beach and at the dune foot on October 7th and October 24th (see Figure 16). The deviating mass flux patterns can probably be explained by upwind morphology parameters, which influence aeolian mass flux path before it reaches the measurement array.

5.2 Influence of the wind conditions

The drag and lift forces that act on the sand particles will increase, when the wind speed increases. When the wind becomes strong enough, sand particles can start moving in the form of creep and saltation (Bagnold, 1941; Houser, 2009; Nickling and Neuman, 2009). In this study, the first

aeolian mass fluxes were observed with wind speeds of 6 m/s, which were almost the same wind speeds compared to the findings by Davidson-Arnott and Law (1990), where they found that the critical shear velocity was 5.9 m/s. The variation might be explained due to that during this study the measurements were done over a bar-trough beach, while in the research of Davidson-Arnott and Law (1990) the measurements were done over a flat beach. Thus the higher critical shear velocity found in this research might be explained by the surface parameters.

Furthermore, the correctness of the method used in the results of plotting the mean wind speed with the mean aeolian mass flux might also be discussed. Because de Vries et al. (2014) state that fluctuations in aeolian mass fluxes can occur in seconds and therefore have a major influence on the amount of aeolian sand transport in down-wind fetch length. However, to get more insight in how aeolian mass fluxes react in seconds, different instruments are needed to measure aeolian mass flux variation in seconds.

Comparing the down-wind aeolian mass flux data measured during this study with the findings done by Davidson-Arnott and Law (1990), it can be noticed that aeolian mass flux trends do not show a similar down-wind pattern during cross-shore and longshore wind directions and during equal wind speeds (see Figure 3, Figure 15, Figure 16 and Figure 17).

5.2.1 Cross-shore wind measurements

During the cross-shore wind conditions measured at the intertidal beach, the upper beach and the dune foot, it can be noticed that aeolian mass fluxes increase in down-wind direction as was also described by Davidson-Arnott and Law (1990) (see section 5.1). However, when comparing the cross-shore aeolian mass fluxes in down-wind distance and the averaged mean wind speed of the measurement location (Figure 17) with the research by Davidson-Arnott and Law (1990). It reveals that aeolian mass flux patterns in down-wind distance approximately match during equal wind speeds. During the measurements on October 22nd, it was noticed that around equal mean wind speeds of approximately 6 m/s (Figure 17), the same aeolian mass fluxes were shown after 10 – 15 meter down-wind distance (Figure 15). These findings can be compared to the lowest mean wind speed measurements in Figure 3. But aeolian mass fluxes measured on April 2nd (Figure 15) cannot be compared to the middle mean wind speed measurements in Figure 3. Because the mean wind speed during that measurement day, which was between 6 – 7.5 m/s (see Table 2) was not equal to the wind speeds found by Davidson-Arnott and Law (1990). In their research they found 0.01 kg m⁻¹ s⁻¹ lower aeolian mass fluxes with wind speeds of 8.5 m/s (Figure 3). This variation in mass flux can probably be explained by the missing wind speed measurements that were made during the run with the sediment catchers on April 2nd (see Figure 10 B). As a consequence of this, the mean wind speed was determined from the known wind speed data measured during the event on April 2nd and might

therefore be lower than actually was. But since there are no other wind speed measurements done during this measurement day, it still cannot be confirmed.

During cross-shore measurements, it was noticed that near the dune foot area a decrease in aeolian mass flux was observed. By only looking at the fetch theory, this decrease in aeolian mass flux could not be explained (see section 5.1). This same decrease in aeolian mass flux was observed in the research by Bauer et al. (2009) and Delgado-Fernandez (2010). Whereupon Bauer et al. (2012) were the first who explained this decrease in aeolian mass flux, with a decrease in wind speed that occurs near the dunes during oblique incoming winds. This explanation is in agreement with the wind speed measurements done during the field campaigns. Because during the oblique wind event on October 22, it was noticed that the wind speeds at the intertidal beach and at the upper beach were higher than the wind speed measurements at the dune foot (see Figure 13 B). Another explanation for the decrease in wind speed near the dunes might be by to the development of an internal boundary layer. This internal boundary layer develops in front of the dunes and leads to a reduction in wind speed (Bauer et al., 2009). In the research of Bauer et al. (2009) they only found this internal boundary layer during onshore wind directions. Furthermore, Bauer et al. (2012) predicted also that during onshore wind conditions most aeolian sand transport will be measured. However in order to confirm both these theories, aeolian sand transport measurements need to be done during onshore wind events, which were not made during the field campaigns.

When looking at what would be the most important factor to start aeolian sand transport over the beach during cross-shore wind conditions, it can be noticed that the wind direction ensures a limiting fetch length and therefore the wind speed is most important for the increase of aeolian mass flux over the beach towards the dunes. Therefore, the hypothesis for the cross-shore wind conditions can be accepted.

5.2.2 Longshore wind measurements

During longshore wind directions, the fetch length can become infinite and aeolian sand transport can reach its saturated condition for the gusting wind (Davidson-Arnott and Law, 1990). However, in section 4.2 it was shown that this saturated condition was not always reached during longshore wind directions. Even when the mean wind speed remained approximately equal during both measurement events on October 7th and October 24th (Figure 17), a difference in aeolian mass flux in down-wind distance can be detected between the measurement arrays during the same event (Figure 16). A possible explanation for the observed variation in down-wind aeolian mass fluxes was given in the research by Bauer et al. (2012), where they state that the smallest change in wind direction, i.e. from longshore towards oblique, can influence the fetch length. This would indicate that the fetch can change from infinite, during longshore wind directions, towards limited during

slightly more oblique wind directions. However, these changes in wind direction were not observed during the measurements done during the field campaigns (see Figure 11 B and Figure 14 B). In these figures it can be noticed that when the wind direction changed, the wind direction became more favourable for infinite fetch lengths during the runs. Another way to explain the variation in aeolian mass flux between the two arrays during the same measurement event is by a variation in the upwind morphology that ensures a limitation in the upwind fetch length. For example, a variation in the upwind beach width can cause a decrease in aeolian mass flux in down-wind direction, which can result in miss-predictions when aeolian mass fluxes towards the dunes are predicted at the field site.

As a consequence of the aforementioned influences, it can be expected that not only the wind direction has the most influence on aeolian mass flux at the upper beach and dune foot area during longshore wind direction, but probably that there are also other important parameters that influences aeolian mass flux in down-wind distance. Therefore, the hypothesis for the longshore wind conditions was probably not complete. However to confirm this more morphological measurements need to be done in upwind direction during longshore wind conditions.

5.2.3 External wind measurements

In order to find out if the wind conditions measured at the nearby weather station De Kooy, Den Helder can be used to predict aeolian mass fluxes at the study site, the average wind data measured at the nearby weather station is shown in Table 3. Comparing the measured wind conditions from this weather station with the measured wind conditions at the beach surface (Table 2), it is shown that the wind conditions at the weather station were relatively higher than at the field site (section 3.5). This difference can be explained by the relatively large distance between the field site and the weather station of 42 km. Furthermore, the wind conditions measured at the weather station were measured at a height of 10 m above the ground, while at the field site these wind conditions were measured at 0.9 m above the ground. This implies that the measured wind speeds at the weather station 'De Kooy' were not accurate enough to give a suitable prediction of the wind speed at the different parts of the beach and therefore cannot be used for predicting aeolian mass fluxes over the beach.

5.3 Influence of the morphology

In the research of Davidson-Arnott et al. (2005) it was shown that due to drying of the beach surface, a dynamic threshold for the start of aeolian sand transport can arise. However, in this study little fluctuations for the surface moisture content were noticed before and after a run (see Figure 18). Therefore in the results there was no correction made for the dynamic process that was caused by the drying of the beach during a run, as was suggested by Davidson-Arnott et al. (2005).

In this study it is expected that the upwind morphology was the same as measured near the sediment catcher array. However, Edwards and Namikas (2009) state that the measured moisture content next to the sediment catchers might not be comparable to the upwind surface moisture content. As a consequence the upwind surface moisture content might be different than expected. In this study these upwind surface moisture content variations were not measured during the field campaigns. However, in future research it is advisable to measure also the upwind surface moisture contents during longshore wind conditions in order to get better aeolian mass flux predictions.

5.3.1 Intertidal beach area

It appears from the results that it is hard to start aeolian sand transport at the intertidal beach. This is caused by relatively large grains, higher surface moisture contents and relatively large elevation variations compared to upper beach area and the dune foot area (see Figure 18 and Figure 19). The high surface moisture contents in this area can be explained by the frequent tidal flooding. During high tide, the intertidal beach was mostly flooded or was located in the swash zone. While during low tide conditions, the troughs will remain quite moist due to the lower beach elevations in comparison to the bar and upper beach (Anthony et al., 2009). Furthermore, the grain size at the bar and trough were relatively large compared to the upper beach and the dune foot area (Figure 18). As a result of the frequent flooding, the grains at the beach surface are mixed and remain poorly sorted (Pedreros et al., 1996). As a result that during favourable wind conditions, the poorly sorted grains are unfavourable to start aeolian sand transport. The high surface moisture content at the intertidal beach area and the larger grains can influence the threshold of movement and therefore aeolian sand transport will be limited (Davidson-Arnott et al., 2005). As a result, different fetch segments might arise over the beach during low tide conditions (Anthony et al., 2009) (see Figure 4). At the bar, aeolian sand transport can arise under the condition that the surface moisture content was low enough, while the trough remains moist and acts as a sediment trap during unfavourable wind conditions. At the moment the wind speed was strong enough aeolian sand transport can move over the trough area and can continue in down-wind direction. As a result, the fetch can increase in down-wind direction. However, no aeolian mass fluxes were measured over the bar-trough system to confirm these aforementioned theories.

During the aeolian event on October 22, measurements of all three parameters were collected at the intertidal beach and are shown in Figure 18 D. In this figure it is noticed that the increase in aeolian mass flux only starts after the surface moisture content became below approximately 10 %. This same influence of the surface moisture content on aeolian mass flux was also observed in the researches by Wiggs et al. (2004), Davidson-Arnott et al. (2008), Anthony et al. (2009) and Bauer et

al. (2009). Where they found aeolian sand transport fluxes when the surface moisture content was approximately 8 %.

In the results no relation was found between the variation of the beach elevation at the intertidal beach and the influence on aeolian mass flux. Because no aeolian mass fluxes were measured over the bar-trough area during the field campaigns to confirm this theory. However, in the research by Anthony et al. (2009) it was stated that over these bar-trough profiles the wind speed may vary in down-wind distance due to air expansion. This might have a large influence on aeolian mass flux that arises over the intertidal area. Therefore, these wind variations in down-wind distance should also be taken in consideration during future fieldwork campaigns, which can be done by placing more sonic anemometers and sediment catchers over the bar-trough beach when aeolian sand transport appears at the intertidal beach. As a result better aeolian sand transport predictions can be made for the intertidal beach area towards the dunes.

5.3.2 Upper beach area

The results show that there was an earlier start in aeolian sand transport at the upper beach compared to the intertidal beach. At the upper beach, almost no elevation variation was noticed and almost no variation in surface moisture content and grain size variation were measured (see Figure 18 B). In this figure one exception was noticed for the third sediment catcher at the upper beach, where relatively larger surface moisture contents were measured. This can be explained by that the measurement location was positioned slightly more towards the sea (see Figure 14 A). Almost no variation in surface parameters are noticed in Figure 18 B and therefore it is assumed that all surface factors are relatively in favour to start or to remain aeolian sand transport into motion in down-wind direction at the upper beach towards the dunes.

5.3.3 Dune foot area

At the dune foot, it is also relatively easy for the wind to start or to remain aeolian sand transport into motion compared to the intertidal beach. However, it is noticed that there are relatively large variations in elevation and slightly larger grain size particles at the dune foot area compared to the upper beach area (see Figure 18), which might result in more unfavourable transport conditions. In Figure 18 C it was noticed that at the moment the elevation increases, a decrease in aeolian mass flux could be noticed. While all other surface parameters remained approximately equal over the beach. This might indicate that the change in beach elevation also had influence on aeolian mass flux. However, not all three surface parameters were continuously measured during the field campaigns to confirm this theory. Another theory might be that there are also other surface parameters that can influence aeolian sand transport (section 2.3), but these surface parameters were not measured

during the field campaigns to confirm this theory. But from the results it can be noticed that at the dune foot area the surface parameters still remain favourable enough for aeolian sand to transport sand fluxes towards the dunes.

5.3.4 Morphology variations through time

In the results it is shown that all the grain size class distributions are highly variable at the intertidal area through time compared to the upper beach and the dune foot area (see Figure 21). At the intertidal area, the fine sand particles were restrained by the larger particles, which make the fine particles less available for aeolian sand transport. During each high tide the intertidal beach was reworked again, which sort the grains poorly (Pedreros et al., 1996). At the upper beach and at the dune foot area no tidal influence occurs, therefore the grains at the beach surface were better sorted and easier to lift during aeolian transport. As a result of the tidal influence, it is harder to start aeolian sand transport from the intertidal area than at the upper beach and dune foot area.

However, for the D_{90} grain size class a larger increasing trend can be observed at the dune foot than for the other two grain size classes (see Figure 21 C). This increase cannot be explained by the tidal influence, but might be explained by the relatively large amounts of aeolian sand transport events that occurred. Therefore, it can be expected that the smaller grains were lifted by the wind and were transported in down-wind direction, with as a consequence that the larger grains remain and therefore a relatively increase in larger grains were observed at the dune foot. But which affect this might have had on aeolian mass flux in down-wind distance is not clear, because the grains that remain at the dune foot remained still quite small (see Appendix, Figure 22 and Figure 23). However, more grain size samples need to be taken before and after aeolian events to get better understanding in how many sand particles are transported. Nevertheless, this variation in grain size classes over the beach should be taken into account when aeolian events are modelled.

6. Conclusions

This study was conducted to get more insight in which factors influence aeolian sand transport over the beach, in order to get a better indication about the amount of sand that is transported towards the dunes. To indicate which factors increase or limit aeolian mass flux over the beach, the beach is divided into three sub-areas.

At the intertidal beach, it is observed that the limiting factor is the morphology. In this study it is shown that the high surface moisture content ensures for moist segments that will prevent or limit the increase of aeolian sand transport in down-wind distance. The grains at the surface are reworked during high tide. As a result the grains will remain poorly sorted, so the larger grains limit the smaller grains to be lift by the wind. During oblique winds the beach width is limited and therefore it will become more difficult for aeolian sand transport to arise, or it will prevent aeolian mass flux to increase to its maximum. However when the wind is strong enough, there is a chance that aeolian mass fluxes are able to arise over the beach. Thus, the wind speed is the most important factor at this beach area.

It is shown that the conditions to start or to continue aeolian sand transport are most favourable at the upper beach. The small variations in the beach morphology ensures for limiting influence on aeolian sand transport. At this part of the beach, the wind direction becomes more important because it will increase the fetch distance. However, when the wind is not strong enough to lift sand particles, no aeolian mass fluxes will arise. Therefore at the upper beach, the combination of fetch length and wind speed ensures for most increase in aeolian mass flux.

At the dune foot, it is noticed that the morphology is slightly more unfavourable than at the upper beach area. This because the D_{90} grain size class is relatively larger and varies more through time. Furthermore, the variation in elevation might also influence aeolian sand transport in down-wind direction. It is also indicated that during oblique wind conditions the wind speed is relatively lower than at the intertidal beach and the upper beach area. This might result again in a limitation in the transport of aeolian sand towards the dunes. The wind direction is most important at the dune foot, because the wind direction will ensure that the fetch is long enough to increase to its maximum.

In order to give better predictions for aeolian sand transport towards the dunes during model studies, it must be considered that there are several factors that increase or limit aeolian sand transport which alternate one another over the beach and through time. Furthermore, in the results it is shown that the wind speed decreases near the dunes during oblique wind directions, which might influence the amount of aeolian sand transport towards the dunes. Therefore all these different increasing or limiting parameters at the different parts of the beach should be taken into account when predicting aeolian sand transport over the beach towards the dunes.

Acknowledgements

I would like to thank my supervisors Winnie de Winter and Gerben Ruessink for their support, ideas, insights, and corrections for my work during the process and completion of this thesis. I want to thank the technical staff of the department of physical geography: Marcel, Henk, Arjen, Bas and Chris. The field campaigns would not be possible without their efforts and knowledge, because they ensured that all the equipment worked well during the field campaigns. Whereupon, I also wanted to thank the fellow fieldwork participants for their efforts and their support during the field campaign and for all the help I received during the data processing: Winnie, Jasper, Pam and Yvonne. Then I would like to thank all the people who helped me to find motivation and creativity, helped me processing the data and for the nice discussions during the coffee breaks: Niels, Jaco and Elise. Finally, I wanted to thank all the people who read my thesis and helped me to improve my English: Jaco, Jessica, Johannes, Ruud, Elise, Jolien and Eva.

References

- Anderson, R.S., 1987. Eolian Sediment Transport as a Stochastic Process : The Effects of a Fluctuating Wind on Particle Trajectories. *J. Geol.* 95, 497–512.
- Anthony, E.J., Ruz, M.H., Vanhée, S., 2009. Aeolian sand transport over complex intertidal bar-trough beach topography. *Geomorphology* 105, 95–105.
- Atherton, R. J., Baird, A. J., & Wiggs, G. F. (2001). Inter-tidal dynamics of surface moisture content on a meso-tidal beach. *Journal of Coastal Research*, 482-489.
- Bagnold, R. A. (1941). *The physics of blown sand and desert dunes*. Chapman and Hall, London, 256 pp.
- Bauer, B.O., Davidson-Arnott, R.G.D., 2002. A general framework for modeling sediment supply to coastal dunes including wind angle, beach geometry, and fetch effects. *Geomorphology* 49, 89–108.
- Bauer, B.O., Davidson-Arnott, R.G.D., Hesp, P. a., Namikas, S.L., Ollerhead, J., Walker, I.J., 2009. Aeolian sediment transport on a beach: Surface moisture, wind fetch, and mean transport. *Geomorphology* 105, 106–116.
- Bauer, B.O., Davidson-Arnott, R.G.D., Walker, I.J., Hesp, P. a., Ollerhead, J., 2012. Wind direction and complex sediment transport response across a beach-dune system. *Earth Surf. Process. Landforms* 37, 1661–1677. doi:10.1002/esp.3306
- Davidson-Arnott, R.G., MacQuarrie, K., Aagaard, T., 2005. The effect of wind gusts, moisture content and fetch length on sand transport on a beach. *Geomorphology* 68, 115–129. doi:10.1016/j.geomorph.2004.04.008
- Davidson-Arnott, R. G.D., & Law, M. N. (1990). Seasonal patterns and controls on sediment supply to coastal foredunes, Long Point, Lake Erie. *Coastal dunes: form and process*, 177-200.
- Davidson-Arnott, R.G.D., Yang, Y., Ollerhead, J., Hesp, P. a., Walker, I.J., 2008. The effects of surface moisture on aeolian sediment transport threshold and mass flux on a beach. *Earth Surf. Process. Landforms* 33, 55–74.
- de Vries, S., Arens, S.M., de Schipper, M. a., Ranasinghe, R., 2014. Aeolian sediment transport on a beach with a varying sediment supply. *Aeolian Res.* 15, 235–244.
- Delgado-Fernandez, I., 2010. A review of the application of the fetch effect to modelling sand supply to coastal foredunes. *Aeolian Res.* 2, 61–70.
- Edwards, B.L., Namikas, S.L., 2009. Small-scale variability in surface moisture on a fine-grained beach: implications for modeling aeolian transport. *Earth Surf. Process. Landforms* 34, 1333–1338.
- Ellis, J.T., Li, B., Farrell, E.J., Sherman, D.J., 2009. Protocols for characterizing aeolian mass-

- flux profiles. *Aeolian Res.* 1, 19–26.
- Gillette, D.A., Herbert, G., Stockton, P.H., Owen, P.R., 1996. causes of the fetch effect in wind erosion. *Earth Surf. Process. Landforms* 21, 641–659.
- Holman, R.A., Stanley, J., 2007. The history and technical capabilities of Argus. *Coast. Eng.* 54, 477–491. doi:10.1016/j.coastaleng.2007.01.003
- Houser, C., 2009. Synchronization of transport and supply in beach-dune interaction. *Prog. Phys. Geogr.* 33, 733–746. doi:10.1177/0309133309350120
- Nickling, W. G., & Neuman, C. M. (2009). Aeolian sediment transport. In *Geomorphology of desert environments* (pp. 517-555). Springer Netherlands.
- Oblinger, A., Anthony, E.J., 2008. Surface Moisture Variations on a Multibarred Macrotidal Beach: Implications for Aeolian Sand Transport. *J. Coast. Res.* 245, 1194–1199.
- Pedreras, R., Howa, H., Michel, D., 1996. Application of grain size rend analysis for the determination of sediment transport pathways in intertidal areas. *Mar. Geol.* 135, 35–49.
- Quartel, S., Ruessink, B.G., Kroon, A., 2007. Daily to seasonal cross-shore behaviour of quasi-persistent intertidal beach morphology. *Earth Surf. Process. Landforms* 32, 1293 – 1307. doi:10.1002/esp
- Sherman, D.J., Li, B., 2012. Predicting aeolian sand transport rates: A reevaluation of models. *Aeolian Res.* 3, 371–378.
- Sterk, G., Parigiani, J., Cittadini, E., Peters, P., Scholberg, J., Peri, P., 2012. Aeolian sediment mass fluxes on a sandy soil in Central Patagonia. *Catena* 95, 112–123.
- Sterk, G., Raats, P. a. C., 1996. Comparison of Models Describing the Vertical Distribution of Wind-Eroded Sediment. *Soil Sci. Soc. Am. J.* 60, 1914.
- van Boxel, J.H., Sterk, G., Arens, S.M., 2004. Sonic anemometers in aeolian sediment transport research. *Geomorphology* 59, 131–147.
- Van Rijn, L. C. (1990). *Principles of fluid flow and surface waves in rivers, estuaries, seas and oceans* (Vol. 11). Amsterdam, The Netherlands: Aqua Publications.
- Vanhée, S., Anthony, E.J., Ruz, M., 2002. Aeolian Sand Transport on a Ridge and Runnel Beach : Preliminary Results from Leffrinckoucke Beach , Northern France. *J. Coast. Res.* 740, 732–740.
- Walker, I.J., 2005. Physical and logistical considerations of using ultrasonic anemometers in aeolian sediment transport research. *Geomorphology* 68, 57–76.
- Wiggs, G.F.S., Baird, a. J., Atherton, R.J., 2004. The dynamic effects of moisture on the entrainment and transport of sand by wind. *Geomorphology* 59, 13–30.
- Yang, Y., Davidson-Arnott, R.G.D., 2005. Rapid Measurement of Surface Moisture Content on a Beach. *J. Coast. Res.* 213, 447–452.

Appendix, additional figures

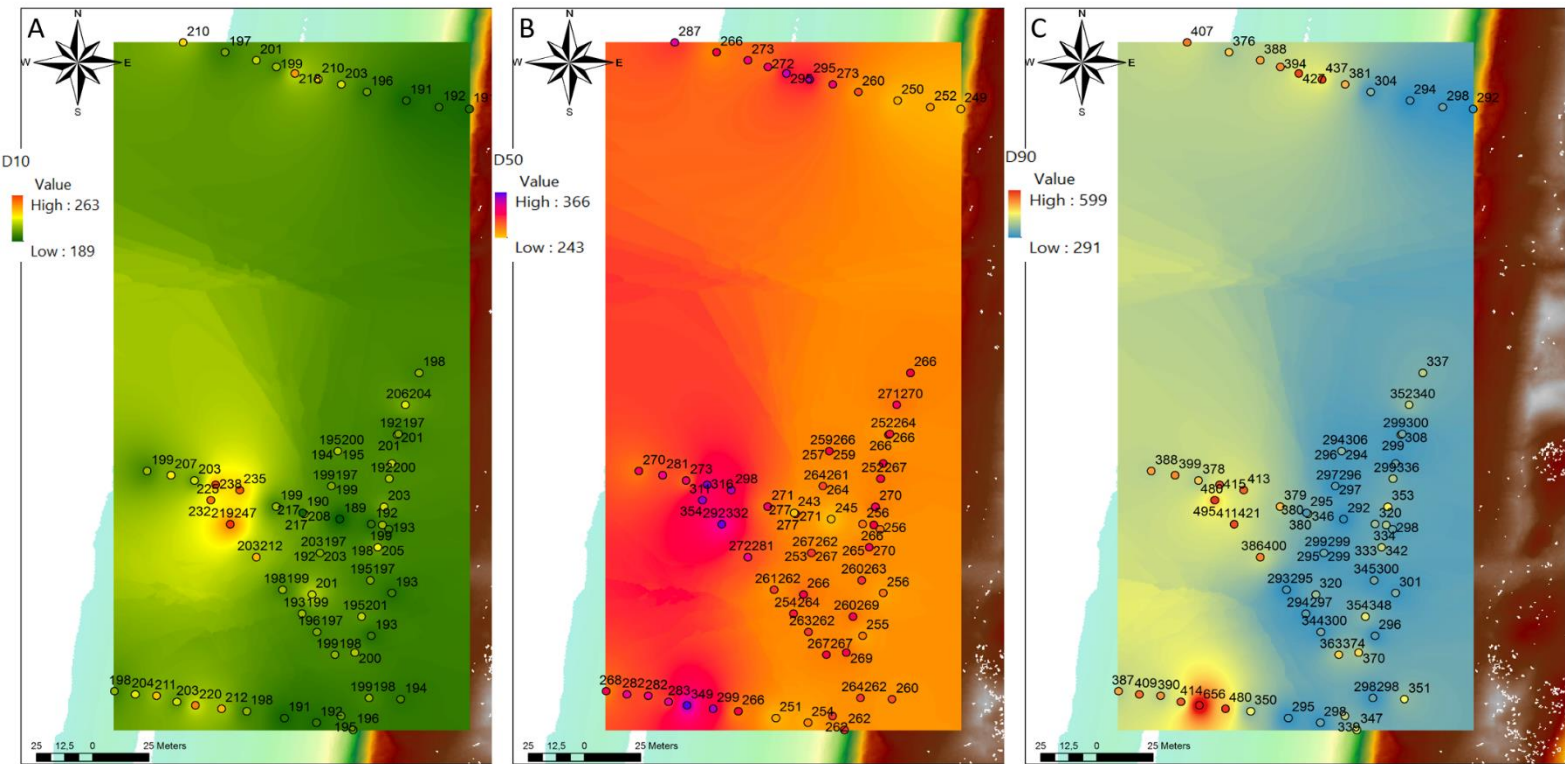


Figure 22: An overview of the grain size distribution achieved by the inverse distance weighting (IDW) interpolation for all the grain size class measurements done between October 19 and October 24. A; the grain size distribution for the D_{10} class. B; the grain size distribution for the D_{50} class. C; the grain size distribution for the D_{90} class. All grain size values are in μm .

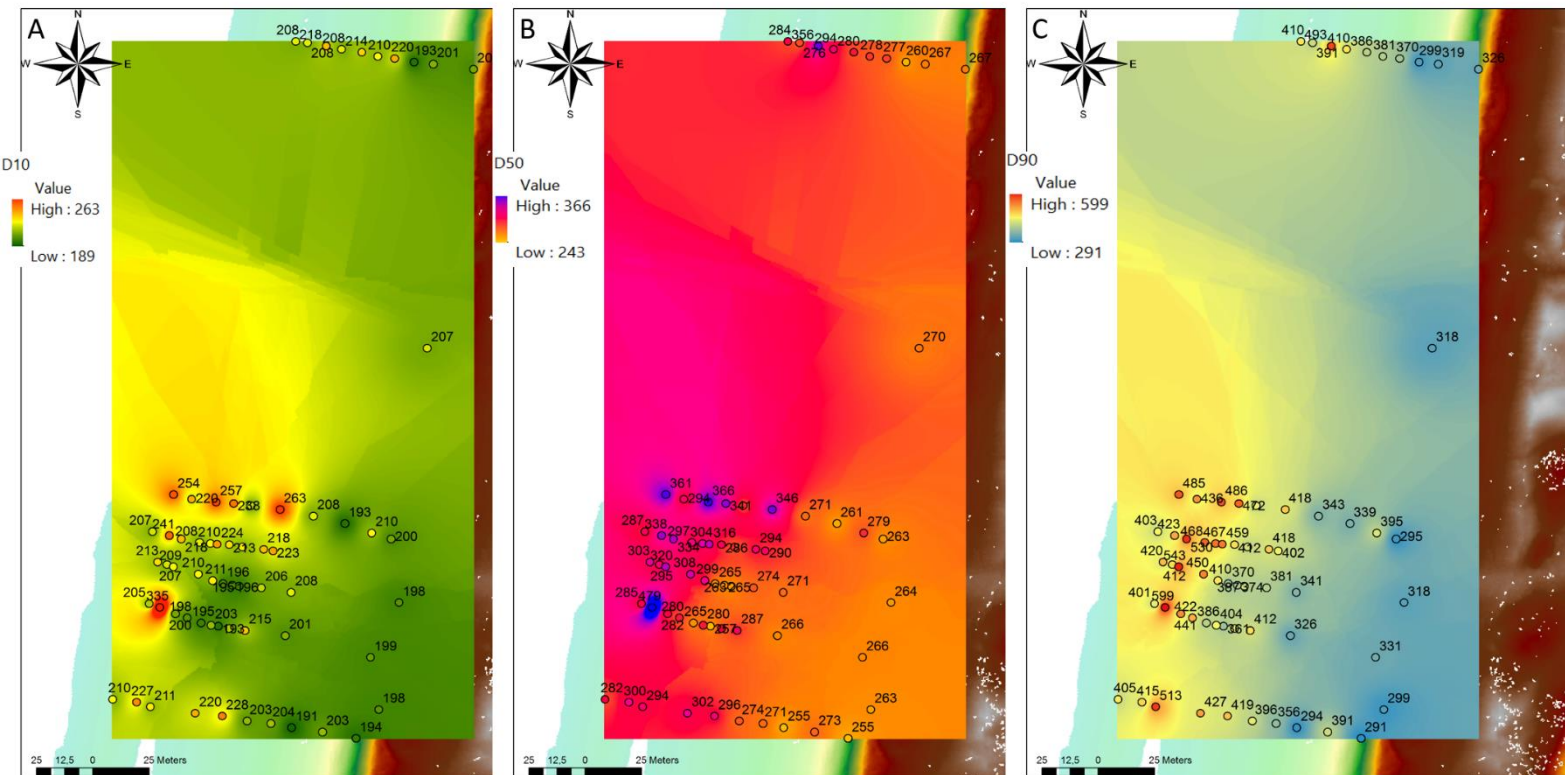


Figure 23: An overview of the grain size distribution achieved by the inverse distance weighting (IDW) interpolation for all the grain size class measurements done between October 27 and October 29. A; the grain size distribution for the D_{10} class. B; the grain size distribution for the D_{50} class. C; the grain size distribution for the D_{90} class. All grain size values are in μm .